# Dissipative effects on quantum glassy systems

L. F. Cugliandolo,[1,2] D. R. Grempel,[3] G. Lozano,[4] H. Lozza,[4] and C. A. da Silva Santos[5]
[1]*Laboratoire de Physique Théorique de l'École Normale Supérieure, 24 rue Lhomond, 75231 Paris Cedex 05, France*
[2]*Laboratoire de Physique Théorique et Hautes Énergies, Jussieu, 1er étage, Tour 16, 4 Place Jussieu, 75252 Paris Cedex 05, France*
[3]*CEA-Saclay/SPCSI, 91191 Gif-sur-Yvette CEDEX, France*
[4]*Departamento de Física, FCEyN, Universidad de Buenos Aires, Pabellón I, Ciudad Universitaria, 1428 Buenos Aires, Argentina*
[5]*Instituto Carlos I de Física Teórica y Computational, Universidad de Granada, E-18071 Granada, Spain*
(Received 30 October 2001; revised manuscript received 19 February 2002; published 22 July 2002)

We discuss the behavior of a quantum glassy system coupled to a bath of quantum oscillators. We show that the system localizes in the absence of interactions when coupled to a sub-Ohmic bath. When interactions are switched on localization disappears and the system undergoes a phase transition towards a glassy phase. We show that the position of the critical line separating the disordered and ordered phases strongly depends on the coupling to the bath. For a given type of bath, the ordered glassy phase is favored by a stronger coupling. Ohmic, sub-Ohmic, and super-Ohmic baths lead to different transition lines. We draw our conclusions from analysis of the partition function using the replicated imaginary-time formalism and from the study of the real-time dynamics of the coupled system using the Schwinger-Keldysh closed time-path formalism.

DOI: 10.1103/PhysRevB.66.014444 PACS number(s): 75.10.Jm, 75.10.Nr, 75.40.Gb

## I. INTRODUCTION

The effects of a dissipative environment on the dynamics of quantum systems have been intensively investigated during the last two decades.[1,2] The most widely studied problem is that of a *single* macroscopic variable coupled to a set of microscopic degrees of freedom that act as a bath. The environment is usually described in terms of its collective excitations (lattice vibrations, spin or charge fluctuations, etc.) that may be thought of as an ensemble of independent quantum harmonic oscillators.[3–7] Their coupling to the system is given in terms of a spectral density $I(\omega) \propto \alpha \omega^s$ for $\omega \ll \omega_c$, where $\alpha$ is a dimensionless coupling constant and $\omega_c$ a high-frequency cutoff. The exponent $s$ characterizes different types of environment. The Ohmic case ($s=1$) is quite generally encountered[2] but super-Ohmic ($s>1$) and sub-Ohmic ($s<1$) baths also occur, e.g., in the case of the Kondo effect in unconventional hosts.[8–10]

The question of how dissipation destroys quantum *coherence*[1,4,5] in two-level systems (TLS's) has been extensively investigated in the literature. The low-energy physics of many tunneling systems is well described by the spin-boson model.[1,2] In this model, the two equivalent degenerate states of the TLS's are represented by the two eigenstates $\sigma_z = \pm 1$ of an Ising pseudospin. A transverse field coupled to $\sigma_x$ (say) represents the tunneling matrix element. Much is known about the properties of this model and its relationship to several other models including the one-dimensional (1D) Ising model with inverse squared interactions,[11] the anisotropic Kondo model,[12,13] or the resonant model.[14] Three different regimes are possible depending on the value of $\alpha$: in the Ohmic case, at zero temperature, there is a phase transition at $\alpha = 1$.[4,5] For $\alpha < 1$ there is tunneling and two distinct regimes develop. If $\alpha < 1/2$, the system relaxes with damped coherent oscillations; in the intermediate region $1/2 < \alpha < 1$ the system relaxes incoherently. For $\alpha > 1$ quantum tunneling is suppressed and $\langle \sigma_z \rangle \neq 0$, signaling that the system remains localized in the state in which it was prepared.

These results also hold for sub-Ohmic baths while weakly damped oscillations persist for super-Ohmic baths.[1] At finite temperatures (but low enough such that thermal activation can be neglected), there is no localization but the probability of finding the system in the state it was prepared decreases slowly with time for $\alpha > \alpha^{CRIT}$.

These conclusions, derived for a *single* TLS interacting with a bath, can be applied to a macroscopic system in the *diluted* regime, *i.e.* when the interactions between the TLS's are unimportant compared with those between a TLS and the bath.[17] There are, however, physical systems that can be viewed as a *dense* set of TLS's in which their mutual interactions can no longer be neglected. The question then arises as to which are the effects of the interplay between the interactions between the TLS's and their coupling to the noise on the physics of the interacting system.

In this paper we discuss this issue in the context of a *glassy* macroscopic system with *random, long-ranged* interactions. This situation is realized experimentally in systems such as uniaxial spin glasses in a transverse magnetic field[18] and disordered Kondo alloys.[19,20] Metallic glasses with tunneling defects are also systems in which the effects that are of interest here could be observed experimentally.

In thermodynamic equilibrium, in the absence of the bath, the interactions between the TLS's lead to the appearance of an ordered state at low enough temperature. If the interactions are of random sign, as in the models we consider here, the latter will be a spin-glass (SG) state. In this phase the symmetry between the states $\sigma_i^z = \pm 1$ at any particular site is broken but there is no global magnetization, $\Sigma_i \langle \sigma_i^z \rangle = 0$. Since the coupling to the bath also tends to locally break the symmetry between the degenerate states of the TLS's, both interactions compete with the tunneling term in the Hamiltonian. We thus expect the presence of noise to increase the stability of the SG state against quantum fluctuations. The consequences of this fact are particularly interesting when the coupling to the bath leads by itself to localization at some $\alpha = \alpha^{CRIT}$. Consider a system of size $N$ with $\alpha > \alpha^{CRIT}$ at $T=0$ and suppose that we turn off the interactions between

 

the TLS's. The ground state of the system is then $2^N$-fold degenerate as each TLS can be in one of the states $\langle \sigma_i^z \rangle = \pm \sigma_0$ (say) independently. If we now turn on an infinitesimal random interaction between the TLS's, this macroscopic degeneracy will be immediately lifted as the system will select among its $2^N$ degenerate configurations the one (or one among the ones) that minimizes the interaction energy. If we denote by $\tilde{J}$ the typical scale of the interactions and by $\alpha^{CRIT}$ the localization threshold, we thus expect a quantum critical point at $\tilde{J}=0$, $\alpha=\alpha^{CRIT}$ between a quantum paramagnet and the ordered state such that, for $\alpha>\alpha^{CRIT}$, the SG phase survives down to $\tilde{J}=0$.

A system of noninteracting localized TLS's and a SG state *in equilibrium* are in some way similar: in both cases $\Sigma_i \langle \sigma_i^z \rangle = 0$ and the presence of order is reflected by a nonvanishing value of the long-time limit of the correlation function, $q_{EA} = \lim_{t\to\infty} N^{-1} \Sigma_i \langle \sigma_i^z(t) \sigma_i^z(0) \rangle$ (since we assume equilibration the correlation is stationary and the reference time can be taken to be zero). However, this resemblance is only superficial. In renormalization-group language, $\tilde{J}$ is a relevant variable.[21] Therefore the details of the dynamics of the two systems are expected to be quite different, in particular the way in which the correlation function reaches its asymptotic limit $q_{EA}$, which determines the low-energy part of the excitation spectrum of the system.

Further differences between the localized state and the SG state are seen from the study of the out-of-equilibrium relaxation of such states. Indeed, an important feature of glassy systems is that their low-temperature dynamics occurs out of equilibrium. If the system is macroscopic, its size $N$ is very large. In a realistic macroscopic situation, the asymptotic long-time limit follows this large-size limit. Many experiments, simulations, and analytical studies show that the time needed to reach equilibrium after entering the glassy phase diverges so quickly that the relevant relaxation occurs out of equilibrium. The dynamics at low temperatures is then nonstationary; i.e., the dynamic correlation functions loose time translation invariance. If $t_w$ denotes the time elapsed since a quench from the high-temperature phase into the SG phase, the symmetrized correlation function $C(t+t_w,t_w)$ depends on both $t$ and $t_w$. The order in which the limits $t_w\to\infty$ and $t\to\infty$ are taken is in this case very important. For sufficiently long $t$ and $t_w$ but in the regime $t \ll t_w$, the dynamics is stationary and the symmetrized correlation function reaches a plateau $q_{EA}$. Much of what was said above for the equilibrium state also holds for this stationary regime. However, for times $t>t_w$, the system enters an *aging* regime where the symmetrized correlation function depends on the waiting time $t_w$ explicitly. In this regime, the symmetrized correlation function vanishes at long times, $\lim_{t\to\infty} C(t+t_w,t_w) = 0$, at a rate that depends on $t_w$. In this regime, even for $\alpha>\alpha^{CRIT}$, small interactions will result in the *destruction* of localization of the TLS's at long enough times.

The problem of a single TLS being a difficult one, that of an infinite set of interacting TLS's seems hardly solvable at this stage. Therefore, as a first step, we shall focus on the low-temperature dynamics of a very simple model that mimics some of the features of more realistic ones. This is a quantum generalization[22–26] of the random $p$-spin spherical model[27] coupled to a bath of quantum harmonic oscillators. The principal merit of this model is that it is simple enough that it can be studied in detail. Yet many of its properties are generic and expected to hold at least qualitatively for more realistic models.[28] The usual methods of equilibrium quantum statistical mechanics are inappropriate to describe the nonstationary situation. We solve the model using two methods especially designed to treat systems out of equilibrium.

One is based on the Schwinger-Keldysh (SK) real-time approach to nonstationary systems. It was first applied in this context to the quantum $p$-spin model in Ref. 23 and used subsequently in other cases including the SU($\mathcal{N}$) fully connected Heisenberg model in the limit of large $\mathcal{N}$ (Ref. 29) and the soft spin version of the Sherrington-Kirkpatrick model.[30] It allows one to obtain the full time dependence of the symmetrized correlation $C(t+t_w,t_w)$.

The second method is based on the *Ansatz* of marginal stability (AMS) within the replica analysis of the partition function. Originally developed for classical systems,[31] this method was recently used to discuss the low-temperature properties of quantum glassy systems.[25,32,33] Its main advantage is that it uses a formalism that is closely related to the imaginary-time approach to equilibrium quantum statistical mechanics. In Ref. 25 the AMS was extensively applied to the quantum spherical $p$-spin model in the absence of the bath. It was shown that the position of the dynamic transition line predicted by this method coincides precisely with that obtained using the real-time approach. It was also shown that the time-dependent correlation function computed using the AMS in the absence of the bath is identical to the *stationary* part of the nonequilibrium symmetrized correlation function ($C>q_{EA}$) when one takes the long-time limit first and the limit in which the coupling to the bath goes to zero next. The marginality condition imposed by the *Ansatz* is intimately related to the fact that the symmetrized correlation will further decay from $q_{EA}$ towards zero. (The details of this second decay as, for instance, the two-time scaling are not accessible with this method.) A localized solution with $C(t+t_w,t_w)$ approaching, and never leaving, the plateau at $q_{EA}$ corresponds, in replica terms, to a stable replica symmetry solution. In this paper we extend the AMS to study the dynamics of the model in the case in which the system is coupled to the environment.

This paper is organized as follows. In Sec. II we motivate and introduce our model and discuss its relationship to the more usual spin-boson model. In Sec. III we outline the imaginary-time formalism used to solve the problem at equilibrium and within the AMS. We compute the partition function of the coupled system and determine its phase diagram in both situations. We also discuss the long-time dynamics of the coupled system using a very accurate long-time approximation[25,26] that allows us to solve the model analytically. This approximation is then used to discuss the influence of a coupling to different types of environment on the $T=0$ quantum phase transition. The real-time dynamics of the system is discussed in Sec. IV and the results are compared with those of Sec. III. Section V contains a brief summary of our main results and our concluding remarks.

## II. MODEL

In order to motivate our model, we start by considering a collection of $N$ identical interacting TLS's coupled to a bath of independent harmonic oscillators.[6,16] We assume for the moment and until otherwise stated that the *combined* system is in thermodynamic equilibrium. The Hamiltonian of the coupled system may be written as

$$H = H_S + H_B + H_{SB}, \tag{2.1}$$

where $H_S$, $H_B$, and $H_{SB}$ denote the Hamiltonians of the system, the bath, and their coupling, respectively. These are given by

$$H_S = -\Delta \sum_{i=1}^{N} \sigma_i^x + V(\sigma_1^z, \sigma_2^z, \ldots, \sigma_N^z), \tag{2.2}$$

$$H_B = \frac{1}{2} \sum_l \left( \frac{p_l^2}{m_l} + m_l \omega_l^2 x_l^2 \right), \tag{2.3}$$

$$H_{SB} = -\sum_{i,l} c_l^i x_l \sigma_i^z. \tag{2.4}$$

Here, the Pauli matrices $\sigma_i^\mu$ represent the TLS's pseudospins, $\Delta/\hbar$ is their tunneling frequency, and $V$ their mutual interaction potential, which we leave unspecified for the moment. $x_l$ and $p_l$ are the coordinate and momentum of the $l$th oscillator and $m_l$ and $\omega_l$ its mass and frequency, respectively. We denote by $c_l^i$ the coupling constant between the $i$th TLS and the $l$th oscillator.

Using standard methods[15,16] the oscillator degrees of freedom may be integrated out to express the partition function of the system solely in terms of the TLS variables as

$$Z \equiv \mathrm{Tr}\, e^{-\beta \hat{H}} = \mathrm{Tr}_{\{\sigma\}} \left[ \mathcal{T} \exp\left( -\frac{S}{\hbar} \right) \right], \tag{2.5}$$

with

$$S = \int_0^{\hbar\beta} d\tau \left\{ -\Delta \sum_i \sigma_i^x(\tau) + V[\vec{\sigma}^z(\tau)] \right\} + \frac{1}{2} \sum_{ij} \int_0^{\hbar\beta} \int_0^{\hbar\beta} d\tau\, d\tau'\, K_{ij}(\tau - \tau') \sigma_i^z(\tau) \sigma_j^z(\tau'), \tag{2.6}$$

where $\mathcal{T}$ is the imaginary-time ordering operator and we have introduced the notation $\vec{\sigma}^z = (\sigma_1^z, \sigma_2^z, \ldots, \sigma_N^z)$.

The kernel $K_{ij}(\tau)$ in Eq. (2.6) is[15]

$$K_{ij}(\tau) = \frac{1}{\hbar\beta} \sum_{\omega_k} \tilde{K}_{ij}(\omega_k) \exp(-i\omega_k \tau), \tag{2.7}$$

where $\omega_k = 2\pi k/(\hbar\beta)$ are the Matsubara frequencies, the coefficients $\tilde{K}_{ij}(\omega_k)$ are given by

$$\tilde{K}_{ij}(\omega_k) \equiv \int_0^\infty \frac{d\omega}{\pi} \frac{I_{ij}(\omega)}{\omega} \frac{\omega_k^2}{\omega^2 + \omega_k^2}, \tag{2.8}$$

and we have introduced the spectral density of the environment $I_{ij}(\omega)$ through

$$I_{ij}(\omega) = \pi \sum_l \frac{(c_l^i c^{j\star}_l + c^{i\star}_l c^j_l)}{2 m_l \omega_l} \delta(\omega - \omega_l). \tag{2.9}$$

We make the simplifying assumption that the dynamic interaction between *different* TLS's generated by integration over the degrees of freedom of the bath can be neglected compared to the static interaction potential included in $V[\vec{\sigma}^z]$. Therefore we write

$$I_{ij}(\omega) = \delta_{ij} I(\omega), \tag{2.10}$$

and we choose the standard parametrization[2]

$$I(\omega) = 2\alpha\hbar \left( \frac{\omega}{\omega_{ph}} \right)^{s-1} \omega e^{-\omega/\omega_c}, \tag{2.11}$$

where $\alpha$ is a dimensionless coupling constant, $\omega_c$ is a high-frequency cutoff, and $\omega_{ph}$ is a microscopic phonon frequency necessary in the non-Ohmic cases in order to keep $\alpha$ dimensionless. For simplicity, we shall restrict the exponent $s$ to lie in the interval $0 < s < 2$. With this choice the integral on the right-hand side of Eq. (2.8) converges without the need of introducing an infrared cutoff and the upper cutoff may be eliminated by taking the limit $\omega_c \to \infty$. This leads to the expression

$$\tilde{K}(\omega_k) = \frac{\alpha\hbar}{\omega_{ph}^{s-1} \sin(\pi s/2)} |\omega_k|^s. \tag{2.12}$$

We shall consider diagonal $p$-spin interactions of the form

$$V[\vec{\sigma}^z] = \sum_{i_1 < \cdots < i_p}^{N} J_{i_1 \cdots i_p} \sigma_{i_1}^z \cdots \sigma_{i_p}^z, \tag{2.13}$$

with random couplings $J_{i_1 \cdots i_p}$. These are taken from a Gaussian distribution with zero mean and variance

$$\overline{(J_{i_1 \cdots i_p})^2} = \tilde{J}^2 p!/(2N^{p-1}), \tag{2.14}$$

where the overline represents an average over disorder.

In the case $p = 2$ and for an Ohmic bath ($s = 1$), Eq. (2.6) is equivalent to the action of a disordered Kondo alloy model.[34] In this context,[13] $\Delta = J_\perp^K$, the transverse Kondo coupling, and $(1 - \alpha) \ll 1$ is proportional to $J_\parallel^K$ the parallel Kondo coupling. In the opposite limit $\alpha \ll 1$, Eq. (2.6) is a representation of the partition function of the SK spin-glass model in a transverse magnetic field[35] weakly coupled to a phonon (or spin[7]) bath.

The main difficulty in solving the quantum statistical mechanical problem defined by Eq. (2.6) stems from the discrete nature of the spins. It was shown by Cugliandolo, Grempel, and da Silva Santos[25] (CGS) that, in the absence of the bath, a solvable (and yet nontrivial) model can be obtained by generalizing the $\sigma^z$ eigenvalues $s_i = \pm 1$ to continuous variables $-\infty < s_i < \infty$ and replacing the hard constraint $s_i^2 = 1$ by the soft spherical constraint $\Sigma_i \langle s_i^2 \rangle = N$. The derivation of the effective continuous model in the presence of

the bath is analogous to that given in CGS for the isolated system and we refer the reader to this reference for the details. After performing a Trotter-like decomposition of the time-ordered exponential in Eq. (2.5) the trace becomes a functional integral over classical fields $s_i(\tau)$ and the tunneling term in the action acquires the low-energy form

$$-\Delta\int_0^{\hbar\beta} d\tau\sigma^x(\tau)\rightarrow\frac{M}{2}\int_0^{\hbar\beta} d\tau\left(\frac{\partial s^z}{\partial\tau}\right)^2, \tag{2.15}$$

where we introduced the *mass*

$$M=\frac{\hbar\tau_0}{2}\ln\left(\frac{\hbar}{\Delta\tau_0}\right), \tag{2.16}$$

and $\tau_0$ is a cutoff representing a microscopic spin-flip time that we identify with $\omega_c^{-1}$. Since we work in the regime in which $\hbar\omega_c$ is the highest energy scale in the problem, $0<M<\infty$.

The continuous version of Eq. (2.6) is thus given by

$$\begin{aligned}S=&\frac{1}{2}\sum_i\int_0^{\hbar\beta} d\tau\left[M\left(\frac{\partial s_i(\tau)}{\partial\tau}\right)^2\right.\\&\left.+\int_0^{\hbar\beta} d\tau'\,K(\tau-\tau')s_i(\tau)s_i(\tau')+\frac{z}{2}[s_i^2(\tau)-1]\right]\\&-\sum_{i_1<\cdots<i_p}^{N}\int_0^{\hbar\beta} d\tau J_{i_1\cdots i_p}s_{i_1}(\tau)\cdots s_{i_p}(\tau),\end{aligned} \tag{2.17}$$

where $z$ is a Lagrange multiplier that enforces the spherical constraint

$$\langle\vec{s}(\tau)\cdot\vec{s}(\tau')\rangle|_{\tau=\tau'}=\frac{1}{\hbar\beta}\sum_k\langle|\vec{s}(\omega_k)|^2\rangle=N, \tag{2.18}$$

where the angular brackets represent the average with respect to the action (2.17). Equations (2.17) and (2.18) define the quantum $p$-spin spherical model that we discuss in the rest of this paper. The mass parameter $M$ is a measure of the strength of quantum tunneling. If $\Delta\tau_0/\hbar\ll 1$, $M$ is large. In this case, the gradient term favors configurations in which $s_i(\tau)$ is almost $\tau$ independent. The partition function is then largely dominated by the contribution from the static fluctuations (i.e., those with $\omega_k=0$). Since $\tilde{K}(\omega_k=0)=0$, these variables are unaffected by the coupling to the bath which drops out of the partition function in this limit. With increasing $\Delta$, $M$ decreases and the amplitude of the quantum fluctuations becomes large. The $\tau$ dependence of $s_i(\tau)$ then becomes essential.

There are three points worth discussing before presenting the solution of the model. The first one is their dependence on the value of $p$. For $p=2$ the action is quadratic and the problem is readily diagonalizable by Fourier transformation. This simple case was extensively discussed in the literature both without[36] and with[34] a bath. In the former case, the competition between the mass and interaction terms in Eq. (2.17) leads to the existence of a critical mass $M_c\sim\hbar^2/\tilde{J}$ above which the ground state of the system overcomes quantum fluctuations and acquires glassy order. For $p=2$, however, the ordered phase is of a trivial type, with a structureless order parameter (see below). Its physical properties are nongeneric and qualitatively different from those of discrete spin systems. The presence of a coupling to the bath does not change this situation. For all $p>2$ the ordered ground state is nontrivial[22–26] and the model shares a number of qualitative features with more realistic ones. Therefore, from here on, we shall discuss this case, choosing the particular value $p=3$ in our numerical calculations.

The second point is about the case $\tilde{J}=0$. In this case Eq. (2.17) reduces to a simplified model for a TLS whose physics differs in some ways from that of real two-level systems. For $\tilde{J}=0$ we have

$$\langle|s(\omega_k)|^2\rangle_{\tilde{J}=0}=\frac{\hbar}{M\omega_k^2+z+\tilde{K}(\omega_k)}, \tag{2.19}$$

where $\tilde{K}(\omega_k)$ is defined in Eq. (2.12) and Eq. (2.18) at $T=0$ reads

$$1=\frac{1}{\pi}\int_0^{\infty} d\omega\,\frac{\hbar}{M\omega^2+\tilde{K}(\omega)+z}\equiv f_s(z). \tag{2.20}$$

We consider the Ohmic case first. For $s=1$, Eq. (2.19) is the propagator of a simple damped harmonic oscillator with frequency $\omega_0=\sqrt{z/M}$ self-consistently determined by Eq. (2.20). From the position of the poles of Eq. (2.19) we see that there is a transition between underdamped and overdamped regimes at $z=\alpha^2\hbar^2/(4M)$. Using this value of $z$ in Eq. (2.20) (with $s=1$) and solving for $\alpha$ we find that this occurs at $\alpha=2/\pi$, independent of $M$. Away from this value we easily find the following limiting behaviors:

$$z=\begin{cases}\dfrac{\hbar^2}{4M}\left(1-\dfrac{4\alpha}{\pi}+\cdots\right), & \alpha\ll 1,\\[2ex] \dfrac{\hbar^2\alpha^2}{M}\exp(-\pi\alpha), & \alpha\gg 1.\end{cases} \tag{2.21}$$

For $\alpha\ll 1$ the system exhibits weakly damped oscillations with frequency $\omega_0\sim\hbar/M$. In the opposite limit $\alpha\gg 1$, the correlation function decays exponentially with a time constant that increases exponentially with the strength of the coupling, $\tau\sim\alpha^{-2}\exp(\pi\alpha)$.

Comparing with the results for the spin-boson model summarized in the Introduction, we see that the transition between coherent and incoherent motion at a universal value of $\alpha<1$ is preserved in the spherical model but the localization transition at $\alpha=1$ is replaced by a crossover to a high coupling regime characterized by an exponentially small energy scale $\propto\exp(-\pi\alpha)$. In this regime, tunneling is not suppressed but its rate is strongly reduced.

In the super-Ohmic case there is no localization transition either. One can easily show that for $s>1$ the expression on the second line of Eq. (2.21) is replaced by $z\sim\hbar\omega_{ph}\alpha^{1/(1-s)}$ for $\alpha\gg 1$. The decay rate of the correlation

function still decreases continuously as the strength of the coupling to the bath increases but only as a power law.

In the case of a sub-Ohmic environment the situation is different. For $s<1$ the integral on the right-hand side of Eq. (2.20) is finite at $z=0$ where it takes its maximum value. For $f_s(0)<1$, Eq. (2.20) cannot be satisfied for any positive value of $z$. This phenomenon, completely analogous to Bose-Einstein condensation, signals a localization transition. Solving the equation $f_s(0)=1$ we find the critical coupling given by

$$\alpha^{CRIT} \sim \left( \frac{\hbar}{M \omega_{ph}} \right)^{1-s}. \tag{2.22}$$

Conversely, for any value of $\alpha$ the system localizes for a sufficiently high value of $M$. These results are analogous to those obtained for discrete TLS's.[1]

One must keep these differences between the original model and its spherical version in mind when interpreting our results, especially those discussed in Sec. III D 2. In Sec. IV we shall illustrate the interplay between the localization observed for $\tilde{J}=0$ and the glassy dynamics that appears when $\tilde{J}>0$.

The third point we want to stress is that the coupled system can be thought as describing the motion of a quantum Brownian particle of mass $M$, constrained to move on a $N$ hypersphere of radius $\sqrt{N}$, in the presence of a random potential $V(\vec{s})$. The Brownian nature of the motion arises because of its interaction with the quantum thermal bath. The infinite-dimensional spherical limit yields, however, nonphysical results if one wants to compare it to the well-known problem of the diffusion of a free quantum particle coupled to a phonon bath in a finite $D$-dimensional space. While here we find a localization transition when the bath is sub-Ohmic, such a transition does not exist in the absence of disorder in the finite-dimensional problem.

## III. REPLICA SOLUTION

It is by now well established that several properties of disordered systems can be derived with the help of the replica trick. This approach enables one to derive an effective action for an imaginary-time-dependent matrix order parameter. It has been noticed that different *Ansätze* that parametrize this order parameter describe different physical situations as thermal equilibrium (equilibrium condition) and the asymptotic dynamic regime (AMS). The bulk of this section is devoted to the analysis of the consequences of the AMS. As discussed in the Introduction we expect that as soon as interactions are switched on, full localization is replaced by a glassy solution with nontrivial dynamics. This argument justifies the use of the AMS from the start. We briefly comment at the end on the equilibrium properties of the model.

### A. Formalism

The presence of disorder makes it necessary to compute the averages of all physical quantities and, in particular, of the free energy. To this effect we use the replica trick; i.e., we write

$$\beta \overline{f} = -\frac{1}{N} \overline{\ln Z} = -\frac{1}{N} \lim_{n \to 0} \frac{1}{n} \ln \overline{Z^n}. \tag{3.1}$$

The derivation of the expression for the free energy associated with the action in Eq. (2.17) closely follows that performed for the isolated system in CGS where the interested reader will find all the necessary details. An imaginary-time-dependent order parameter $Q_{ab}(\tau,\tau')$ is defined as

$$Q_{ab}(\tau,\tau') = \frac{1}{N} \overline{\langle \vec{s}_a(\tau) \cdot \vec{s}_b(\tau') \rangle}, \tag{3.2}$$

where $a,b$ are replica indices. The spherical constraint imposes the restriction $Q_{aa}(0)=1$. We are interested in a stationary situation in which $Q_{ab}(\tau,\tau')$ depends only on time differences and is a periodic function of its argument with period $\beta\hbar$. We thus introduce the Fourier transforms $\tilde{Q}_{ab}(\omega_k) = \int_0^{\hbar\beta} d\tau Q_{ab}(\tau) \exp(i\omega_k)$ in terms of which the averaged free energy is found as

$$\beta \overline{f} = \lim_{n \to 0} G_0, \tag{3.3}$$

where

$$\begin{aligned} 2G_0 = & -\frac{1}{n} \sum_k \mathrm{Tr} \ln[(\beta\hbar)^{-1} \tilde{\mathbf{Q}}] \\ & - \sum_k \left( 1 - \frac{i}{n\hbar} \sum_{ab} \tilde{O}_{ab}(\omega_k) \tilde{Q}_{ab}(\omega_k) \right) - \frac{\tilde{J}^2 \beta}{2\hbar n} \\ & \times \sum_{ab} \int_0^{\beta\hbar} d\tau \left( \frac{1}{\hbar\beta} \sum_k \exp(-i\omega_k \tau) \tilde{Q}_{ab}(\omega_k) \right)^p - \beta z, \end{aligned} \tag{3.4}$$

and the operator $\tilde{O}_{ab}(\omega_k)$ is defined by

$$\tilde{O}_{ab}(\omega_k) \equiv -i\delta_{ab}[M\omega_k^2 + z + \tilde{K}(\omega_k)]. \tag{3.5}$$

The equations of motion are found from the saddle point of the free energy with respect to variations of $\tilde{Q}_{ab}(\omega_k)$. They read

$$\begin{aligned} & \frac{1}{\hbar}[M\omega_k^2 + z + \tilde{K}(\omega_k)]\delta_{ab} \\ & \quad = (\tilde{\mathbf{Q}}^{-1})_{ab}(\omega_k) + \frac{\tilde{J}^2 p}{2\hbar^2} \int_0^{\hbar\beta} d\tau \exp(i\omega_k \tau) Q_{ab}^{p-1}(\tau). \end{aligned} \tag{3.6}$$

Equation (3.6) together with the spherical constraint $Q_{aa}(\tau=0)=1$ determines the different phases in the model.

In the following, we discuss the solutions to Eq. (3.6). Except when otherwise stated, we shall work with dimensionless variables. These are defined by measuring energies in units of $\tilde{J}$ and time in units of $\hbar/\tilde{J}$. The strength of quantum tunneling and of the coupling to the bath are then measured by the parameters

$$\Gamma \equiv \frac{\hbar^2}{(\tilde{J}M)}, \quad \alpha_s \equiv \frac{\alpha}{\sin(\pi s/2)} \left( \frac{\hbar \omega_{ph}}{\tilde{J}} \right)^{1-s}, \tag{3.7}$$

respectively.

In the paramagnetic phase (PM), $Q_{ab}(\omega_k)$ is a diagonal matrix,

$$\tilde{Q}_{ab}(\omega_k) = \tilde{q}_d(\omega_k)\,\delta_{ab}\,. \tag{3.8}$$

Equation (3.6) then reduces to

$$\frac{\omega_k^2}{\Gamma} + z + \alpha_s |\omega_k|^s = \frac{1}{\tilde{q}_d(\omega_k)} + \frac{p}{2}\int_0^\beta d\tau \exp(i\omega_k \tau) q_d^{p-1}(\tau). \tag{3.9}$$

In the SG phase, we search for one-step replica symmetry breaking (RSB) solutions of the form

$$\tilde{Q}_{ab}(\omega_k) = [\tilde{q}_d(\omega_k) - q_{EA}] + q_{EA}\epsilon_{ab}\,, \tag{3.10}$$

where $\epsilon_{ab}=1$ if $a$ and $b$ belong to the same diagonal block of size $m \times m$ and zero otherwise, and we introduced the Edwards-Anderson order parameter $q_{EA}$. It was shown in CGS that this *Ansatz* is an *exact* solution of the isolated model. The proof still holds in the presence of the bath provided that $\lim_{\omega \to 0} \tilde{K}(\omega) = 0$, which is verified here [cf. Eq. (2.12)].

To completely determine the order-parameter matrix, $q_{EA}$ and $m$ must be computed. As discussed in detail in CGS, this may be done in two different ways, each leading to a physically different state. Within the *Ansatz of marginal stability*, $q_{EA}$ is determined by extremization of the free energy and $m$ is chosen such that the stability of the ordered state is marginal, i.e., that its excitation spectrum contains a zero-energy mode.

Decomposing the diagonal order parameter $\tilde{q}_d(\omega)$ in a singular and a regular part,

$$\tilde{q}_d(\omega_k) = \beta q_{EA} \delta_{\omega_k,0} + \tilde{q}_{REG}(\omega_k), \tag{3.11}$$

an equation for $\tilde{q}_{REG}(\omega_k)$ can be derived by a straightforward generalization of the results of CGS to the case in which noise is present. It reads

$$\left[ \frac{\omega_k^2}{\Gamma} + z' + \alpha_s |\omega_k|^s - [\tilde{\Sigma}_{REG}(\omega_k) - \tilde{\Sigma}_{REG}(0)] \right] \tilde{q}_{REG}(\omega_k) = 1, \tag{3.12}$$

with

$$z' = \frac{p}{2} \beta m\, q_{EA}^{p-1} \frac{1+x_p}{x_p}, \tag{3.13}$$

$$\beta m = (p-2) \sqrt{\frac{2}{p(p-1)}} q_{EA}^{-p/2}, \tag{3.14}$$

$$\beta \frac{q_{EA}}{\tilde{q}_d(0)} = \frac{x_p}{m + x_p}, \tag{3.15}$$

and

$$\tilde{\Sigma}_{REG}(\omega_k) = \frac{p}{2}\int_0^\beta d\tau [q^{p-1}(\tau) - q_{EA}^{p-1}] \cos(\omega_k \tau). \tag{3.16}$$

The parameter $x_p$ takes the value

$$x_p = p - 2. \tag{3.17}$$

For given $p$ and $\alpha$, Eqs. (3.12)–(3.16) have solutions with $q_{EA} \neq 0$ only for low enough values of $\Gamma$ and $T$. Otherwise, thermal or quantum fluctuations destroy the ordered state. There is thus a boundary $\Gamma_c(T)$ in the $T$-$\Gamma$ above which the system is in the PM state. We determine its shape below.

### B. Dynamic phase diagram

We determined the phase diagram for the coupled system for $p=3$ using the numerical methods described in CGS. A critical line with a second-order section [close to the classical critical point $(T_d, \Gamma = 0)$] and a first-order section [close to the quantum critical point $(T=0, \Gamma_d)$] is also obtained in the presence of an environment. The second-order critical line is determined by the condition $m=1$; the first-order critical line is defined as the locus of the points where a marginally stable solution first appears with decreasing $\Gamma$ for $T$ fixed (see Fig. 3). For each $\Gamma$ and $\alpha$ this defines a *dynamic* transition temperature $T_d(\Gamma, \alpha)$. It was shown in CGS that $T_d(\Gamma, \alpha)$ precisely coincides with the temperature below which the real-time dynamics of the system loses time-translation invariance and the fluctuation-dissipation theorem (FDT) is violated.[23]

The qualitative features of the phase diagram, similar to those found for the isolated system, are as follows. For $p > 2$, the transition is *discontinuous* in the sense that the order parameter $q_{EA}$ jumps across the phase boundary. The transition line contains a *tricritical point* $(T^\star, \Gamma^\star)$ that divides it into two sections. For $T \geqslant T^\star$, physical properties are *continuous* across the transition. The latter is therefore *second order* in the thermodynamic sense. For $T < T^\star$, instead, physical quantities are *discontinuous* across the transition which is thus *first order*. The origin of this behavior is the fact that the values taken by the parameter $m$ on the transition line are different above and below $T^\star$. For $T > T^\star$, $m = 1$ along the transition line. This is its value in the paramagnetic phase, meaning that $m$ is continuous across the transition and so are the observables. For $T < T^\star$, $m \neq 1$ along the transition line but it is a decreasing function of $T$ that vanishes linearly as $T \to 0$. Crossing the phase boundary at $T < T^\star$, $m$ is discontinuous and so are physical properties.

We show on the right panel of Fig. 1 the dynamic phase

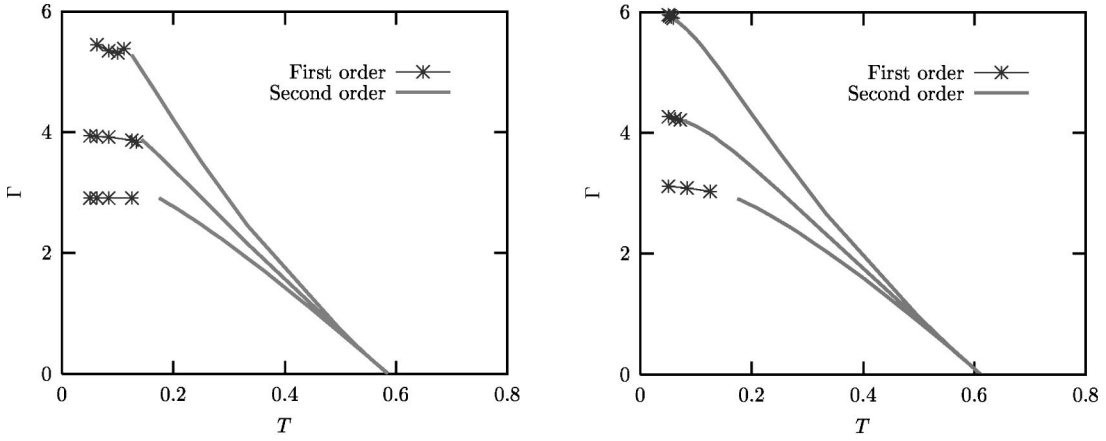


FIG. 1. Static (left) and dynamic (right) phase diagrams for the $p=3$ spin model coupled to an Ohmic bath ($s=1$). The couplings to the bath are $\alpha=$ 0, 0.25, and 0.5 from bottom to top. The solid line and line points represent second- and first-order transitions, respectively.

diagrams obtained for $p=3$ and three values of the coupling to an Ohmic bath, $\alpha=0,0.25,0.5$. The solid line and the line points represent second- and first-order transitions, respectively. We make the following observations.

(i) In the limit $\Gamma\to 0$ the transition temperature is independent of the strength of the coupling to the bath.

(ii) The size of the region in phase space where the system is in the ordered state increases with $\alpha$. Coupling to the dissipative environment thus stabilizes this state.

(iii) The dynamic tricritical temperature decreases rapidly with increasing $\alpha$.

Our first observation is a consequence of the fact that in the limit $\Gamma\to 0$ the partition function is essentially determined by the zero-frequency components of the pseudospin which are decoupled from the bath (see Sec. II). This result is, however, nontrivial from a dynamical point of view, since it implies that the dynamic transition of a classical system coupled to a bath with non-$\delta$ correlations (''colored'' bath) is not modified by the latter.

The second feature follows from simple physical considerations. The interaction term in the action favors spin-glass order. Coupling to the bath favors localization and its effect is to reduce the effective tunneling frequency. Therefore, in the presence of the bath, the value of the bare tunneling frequency needed to destroy the ordered state must increase with $\alpha$. Even if the localized state and the glassy state may seem superficially similar, they are indeed very different. In the former, the symmetrized correlation function $C(t+t_w,t_w)$ approaches a plateau as a function of $t$ and never decays towards zero while in the latter the relaxation first approaches a plateau but it eventually leaves it to reach zero for $t\gg t_w$. We shall see this difference explicitly in the analysis of the real-time dynamics of Sec. IV.

The fact that the coupling to the environment favors the ordered state also reflects itself in the value taken by the order parameters $q_d(\tau)$ and $q_{EA}$. We display in Fig. 2 the $\tau$ dependence of the diagonal part of the order parameter $q_d(\tau)$ for the static and dynamic solutions at a fixed temperature and $\Gamma$ for different values of $\alpha$. It can be seen that, as $\alpha$ increases, $q_d(\tau)$ reaches a higher plateau level at long imaginary times. The analysis of $q_{EA}$ is postponed to Sec. III D.

Figure 3 displays the $m$ dependence of $\Gamma$ at a fixed temperature ($T<T^\star$), for different values of the coupling to the noise. The function $\Gamma(m)$ is double valued and the physical branch is that on which $dm/d\Gamma>0$. This is a consequence of Eq. (3.13), which shows that $m$ is a decreasing function of $q_{EA}$ which itself is a decreasing function of $\Gamma$. It can be seen

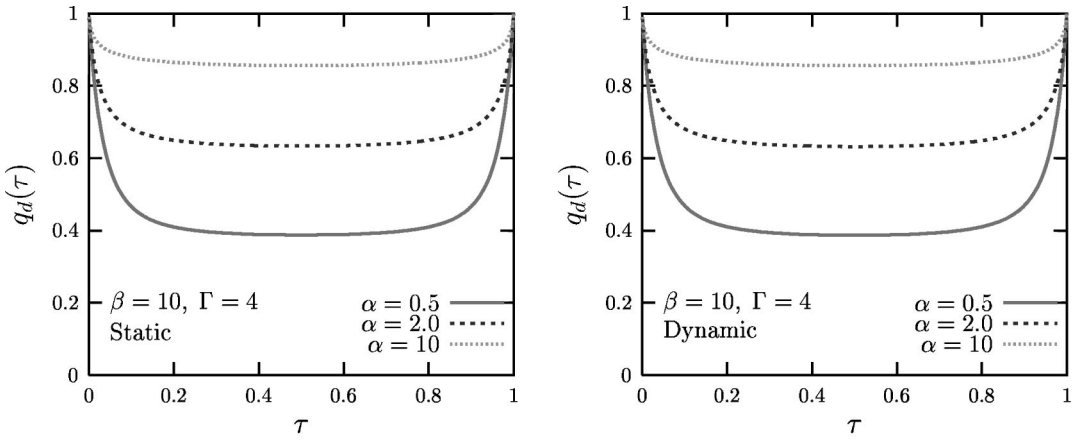


FIG. 2. The diagonal part $q_d(\tau)$ for the static (left) and dynamic (right) solutions.

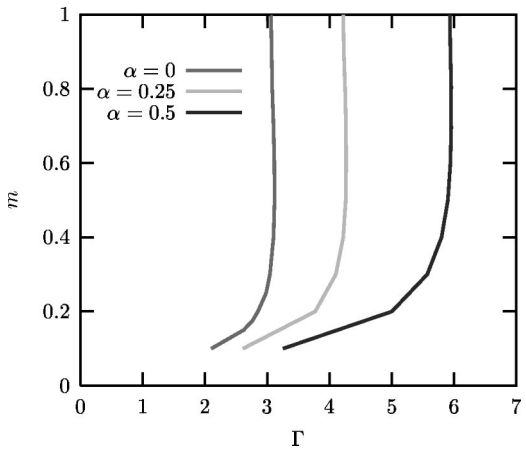


FIG. 3. The break point $m$ as a function of $\Gamma$ for three values of the coupling to an Ohmic environment $\alpha$. $\beta = 20 > \beta^\star$.

that for fixed $\Gamma$ and $T$, $m$ decreases with increasing $\alpha$. Thus, the coupling to the bath results in a higher effective temperature in the glassy phase (see Sec. IV for a definition of $T_{EFF}$ and a discussion on this issue).

We have also studied the phase diagram in the non-Ohmic cases. Figure 4 shows a comparison of the effects of an Ohmic bath and two non-Ohmic ones, sub-Ohmic ($s = 1/2$), and super-Ohmic ($s = 3/2$) for the same value of $\alpha$. It may be seen that for the chosen values of the parameters the region of stability of the ordered phase is enhanced (reduced) for a sub-Ohmic (super-Ohmic) bath with respect to an Ohmic one. This feature is not generic as there are other values of $\omega_{ph}$ for which the relative sizes of the effects of Ohmic and non-Ohmic baths are different. Indeed, in preparing these figures we used $\omega_{ph} = 10$ in the non-Ohmic cases and this parameter modifies the coupling to the bath due to the factor $\omega_{ph}^{s-1}$ in $I(\omega)$.

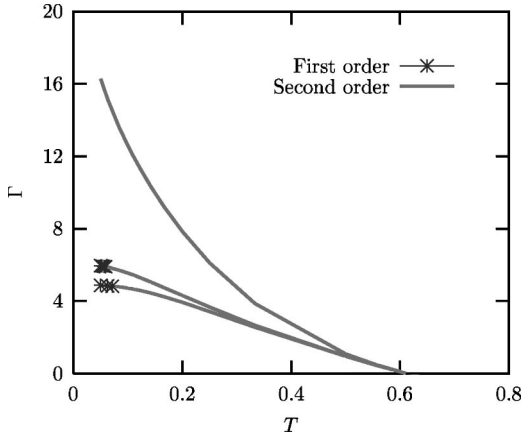


FIG. 4. The dynamic critical line for sub-Ohmic ($s = 1/2$, upper curve), Ohmic ($s = 1$, middle curve), and super-Ohmic ($s = 1.5$, lower curve) baths. $\hbar\omega_{ph}/\tilde{J} = 10$ in the non-Ohmic cases. The dimensionless coupling to the bath is $\alpha = 0.5$ in all cases.

### C. Equilibrium phase diagram

In thermodynamic equilibrium both $q_{EA}$ and $m$ are determined by imposing that the free energy be an extremum with respect to their variation. This leads to the conventional thermodynamic equilibrium state. The value of $x_p$ is obtained from

$$\frac{x_p^2}{p(1+x_p)} - \ln(1+x_p) + \frac{x_p}{(1+x_p)} = 0. \tag{3.18}$$

The transition line is defined as the locus of the points where the free energies of the PM and SG phases coincide. For each $\Gamma$ and $\alpha$ this defines a freezing temperature $T_s(\Gamma,\alpha)$ at which the system enters the SG state. The qualitative features of the equilibrium phase diagram shown on the left panel of Fig. 1 are similar to those found for the dynamic case. Notice that the line $T_d(\Gamma,\alpha)$ lies always *above* $T_s(\Gamma,\alpha)$ and that, in contrast to what we found for the dynamic tricritical temperature, the equilibrium tricritical temperature $T^\star$ depends only weakly on the strength of the coupling to the bath.

### D. Low-energy properties of the marginal SG state

Insights into the low-energy properties of the model may be gained by studying it in the framework of a simple and accurate approximation applied to the isolated model in CGS. It consists in deriving the exact low-frequency form of $\tilde{q}_{REG}(\omega_k)$ and using it over the whole frequency range assuming that physical properties at low temperatures are mainly determined by the low-energy excitations of the system. We consider in the following the $T = 0$ case.

#### *1. Low-frequency form of $\tilde{q}_{REG}(\omega_k)$*

We start by assuming (and verifying later) that $q_{REG}(\tau)$ [cf. Eq. (3.11)] decays in imaginary time as a power law:

$$q_{REG}(\tau) \propto |\tau|^{-\zeta}. \tag{3.19}$$

Then, we may write [cf. Eq. (3.16)]

$$\begin{aligned}\tilde{\Sigma}_{REG}(\omega_k) - \tilde{\Sigma}_{REG}(0) &= \frac{p}{2}\int_0^\beta d\tau (\cos\omega_k\tau - 1) \\ &\quad \times [(p-1)q_{EA}^{p-2} q_{REG}(\tau) + \cdots] \\ &\propto |\omega_k|^{\zeta-1}(1+\cdots),\end{aligned} \tag{3.20}$$

where the ellipsis represents terms that vanish in the limit $\omega_k \to 0$. Therefore, in the long-time limit,

$$\begin{aligned}&\tilde{\Sigma}_{REG}(\omega_k) - \tilde{\Sigma}_{REG}(0) \\ &\quad \approx \frac{p(p-1)}{2} q_{EA}^{p-2} [\tilde{q}_{REG}(\omega_k) - \tilde{q}_{REG}(0)].\end{aligned} \tag{3.21}$$

Substituting Eq. (3.21) in Eq. (3.12) and solving for $\tilde{q}_{REG}(\omega_k)$ we find

$$\tilde{q}_{REG}(\omega_k)=\frac{2}{\omega_k^2/\Gamma+\alpha_s|\omega_k|^s+2\kappa_p+\sqrt{\omega_k^2/\Gamma+\alpha_s|\omega_k|^s}\sqrt{\omega_k^2/\Gamma+\alpha_s|\omega_k|^s+4\kappa_p}}, \tag{3.22}$$

where we introduced the parameter

$$\kappa_p\equiv\sqrt{\frac{p(p-1)q_{EA}^{p-2}}{2}}. \tag{3.23}$$

Equation (3.22) is exact in the low-frequency limit where it reduces to

$$\tilde{q}_{REG}(\omega_k)=\kappa_p^{-1}\left[1-\frac{1}{\sqrt{\kappa_p}}(\omega_k^2/\Gamma+\alpha_s|\omega_k|^s)^{1/2}\right]$$
$$\to\kappa_p^{-1}\left[1-\sqrt{\frac{\alpha_s}{\kappa_p}}|\omega_k|^{s/2}\right]. \tag{3.24}$$

This leads to the long-$\tau$ behavior

$$q_{REG}(\tau)\sim\sqrt{\frac{\alpha_s}{\kappa_p^3}}\frac{1}{|\tau|^{1+s/2}}. \tag{3.25}$$

The assumption (3.19) is thus self-consistent with the exponent $\zeta=1+s/2$. In the absence of the bath Eq. (3.22) leads to

$$q_{REG}(\tau)\sim\frac{1}{\sqrt{\Gamma\kappa_p^3}}\frac{1}{|\tau|^2}, \tag{3.26}$$

the result found previously in CGS for the isolated system. A crossover between these two regimes occurs at $\tau_{cr}=(\Gamma\alpha_s)^{1/(s-2)}$. The analytic continuation of Eq. (3.24) yields the low-frequency limit of the imaginary part of the susceptibility:

$$\chi''_{REG}(\omega)\sim\mathrm{sgn}(\omega)\left(\frac{\alpha_s}{\kappa_p^3}\right)^{1/2}|\omega|^{s/2}. \tag{3.27}$$

The result for the Ohmic case, $\chi''_{REG}(\omega)\propto|\omega|^{1/2}$, was previously found for $p=2$ continuous and discrete Kondo-alloy models at the quantum critical point.[34] In the marginally stable state, this behavior persists throughout the low-temperature phase.

Equation (3.22) is also exact as $\omega_k\to\infty$ where it reduces to $\tilde{q}_{REG}(\omega_k)\sim\Gamma/\omega_k^2$. Therefore, we expect it to be a reasonable interpolation in the whole frequency range. It will be seen in the following that this approximation allows one to gain useful insight into the effects of the environment on the physics of the interacting system.

#### *2. Quantum phase transition*

The normalization condition and Eq. (3.11) lead to the following equation for the order parameter $q_{EA}$ at $T=0$:

$$1-q_{EA}=\frac{1}{\beta}\sum_{\omega_k}\tilde{q}_{REG}(\omega_k)\to_{T=0}\int_{-\infty}^{\infty}\frac{d\omega}{2\pi}\tilde{q}_{REG}(\omega). \tag{3.28}$$

This is still an implicit equation for the order parameter as $\tilde{q}_{REG}(\omega)$ depends on $q_{EA}$ through $\kappa_p$ [cf. Eq. (3.23)].

We now approximate Eq. (3.28) by assuming that the integral on the right-hand side is dominated by the low frequencies. Then, we use for $q_{REG}(\omega)$ the expression given in Eq. (3.22) and write

$$1-q_{EA}=\frac{2}{\pi}\int_0^{\infty}\frac{d\omega}{\omega^2/\Gamma+\alpha_s\omega^s+2\kappa_p+\sqrt{\omega^2/\Gamma+\alpha_s\omega^s}\sqrt{\omega^2/\Gamma+\alpha_s\omega^s+4\kappa_p}}. \tag{3.29}$$

It is convenient to make the change of variables $\omega=(\Gamma\alpha_s)^{1/(2-s)}x$ in Eq. (3.29) which leads to

$$A_s(1-q_{EA})=\int_0^{\infty}\frac{dx}{x^2+x^s+2\epsilon+\sqrt{x^2+x^s}\sqrt{x^2+x^s+4\epsilon}}$$
$$\equiv g_s(\epsilon), \tag{3.30}$$

where

$$A_s=\frac{\pi}{2}(\Gamma^{s-1}\alpha_s)^{1/(2-s)}$$
$$=\frac{\pi}{2}\left(\frac{\hbar}{M\omega_{ph}}\right)^{(s-1)/(2-s)}\left(\frac{\alpha}{\sin\pi s/2}\right)^{1/(2-s)}, \tag{3.31}$$

$$\epsilon=\frac{\kappa_p}{(\Gamma^s\alpha_s^2)^{\frac{1}{2-s}}}=\frac{J}{\hbar}\omega_{ph}\left[\left(\frac{\hbar}{M\omega_{ph}}\right)^s\frac{\alpha^2}{\sin^2\pi s/2}\right]^{1/(s-2)}\kappa_p. \tag{3.32}$$

Equation (3.30) will be used to study the $T=0$ quantum phase transition. We shall mostly be interested in the vicinity of the quantum transition where the system is close to the quantum paramagnetic state. We discuss separately different types of environment.

*a. Ohmic case.* Setting $s=1$ in Eq. (3.30) the equation of state may be written as

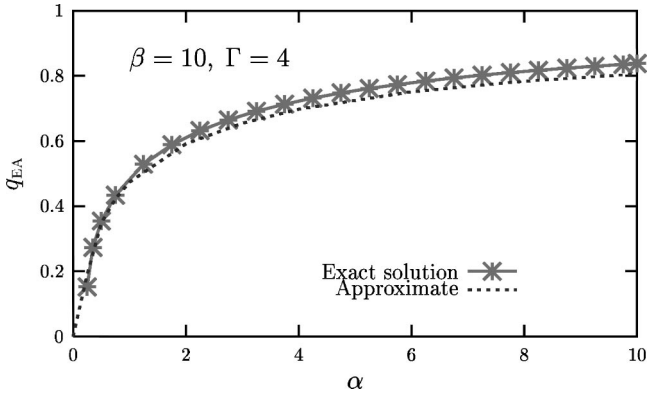


FIG. 5. The dynamic Edwards-Anderson parameter as a function of the coupling to an Ohmic bath, $\alpha$, for $\Gamma=4$ and $\beta=10$. Solid line with point: exact numerical calculations. Dashed line: the low-frequency approximation of Eq. (3.29).

$$\frac{\pi\alpha}{2}(1-q_{EA})=\int_0^\infty \frac{dx}{x^2+x+2\epsilon+\sqrt{x^2+x}\sqrt{x^2+x+4\epsilon}} \equiv g_1(\epsilon), \tag{3.33}$$

with $\epsilon=\kappa_p/(\Gamma\alpha^2)$.

We show in Fig. 5 the $\alpha$ dependence of $q_{EA}$ in the marginally stable case for $p=3$ at fixed $\Gamma=4$. We represent with line points the results obtained numerically from the full equations at a finite but low temperature, $T=0.1$. The dashed line instead represents the approximate solution derived from Eq. (3.29). The agreement between the two calculations is very good even if the approximation strictly applies to the zero temperature case only.

Figure 6 shows $\Gamma$ as a function of $q_{EA}$ for $p=3$ and several values of $\alpha$ as obtained from the numerical solution to Eq. (3.33). The $T=0$ transition takes place at the maximum value of $\Gamma$, $\Gamma_d$. The corresponding value of $q_{EA}$ is the discontinuity of the order parameter at the first-order transition. While $\Gamma_d$ increases rapidly with $\alpha$, the jump of the order parameter *decreases* as the strength of the coupling to the bath increases. The presence of the Ohmic bath thus tends to make the first-order transition smoother. (This property tells us that it will be very difficult to see the first order transition by solving numerically the real-time dynamic equations.)

This behavior results from the fact that $g_1(\epsilon)$ diverges logarithmically as $\epsilon\to 0$. In order to see this, we decompose the interval of integration into two parts $0\leqslant x\leqslant 1$ and $1\leqslant x\leqslant\infty$. The integral over the second interval is a finite constant at $\epsilon=0$. In the integral over the first interval we may neglect $x^2$ compared to $x$ and write

$$\frac{\pi\alpha}{2}(1-q_{EA})\widetilde{\epsilon\to 0}\int_0^1 \frac{dx}{x+2\epsilon+\sqrt{x}\sqrt{x+4\epsilon}} = -\frac{1}{2}\ln\epsilon+\mathcal{O}(1). \tag{3.34}$$

We choose $p=3$ for concreteness and solve Eq. (3.34) for $\Gamma$ to obtain the equation of state in the high-noise limit:

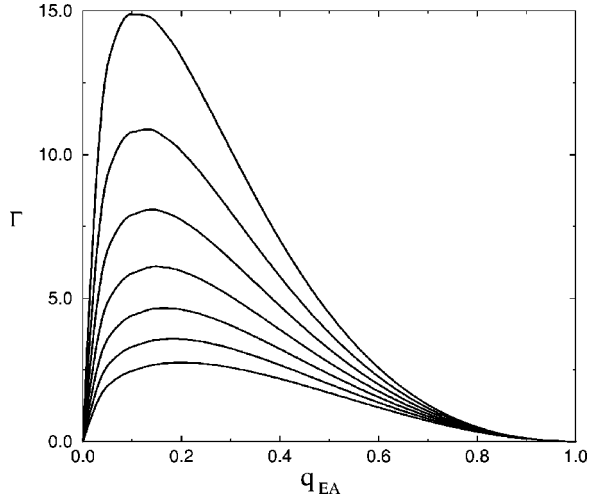


FIG. 6. $\Gamma$ as a function of $q_{EA}$ at $T=0$ for $p=3$ and an Ohmic bath. The curves follow from the numerical solution to Eq. (3.33). The coupling to the bath $\alpha$ runs from 0 to 1.2 in intervals of 0.2 from bottom to top.

$$\Gamma=\frac{1}{\alpha^2}\sqrt{3q_{EA}}e^{\pi\alpha(1-q_{EA})}. \tag{3.35}$$

This function has a maximum at

$$q_{EA}^{\star}\approx\frac{1}{2\pi\alpha}, \tag{3.36}$$

where $\Gamma$ reaches the value

$$\Gamma_{\max}\equiv\Gamma_d\approx\sqrt{\frac{3}{2\pi\alpha^5}}\exp\pi\alpha. \tag{3.37}$$

We thus find the two features mentioned above: namely, a reduction of the discontinuity of the order parameter and a rapid increase of $\Gamma_d$ for high values of $\alpha$. Expressing Eq. (3.37) in terms of the original variables of the problem [cf. Eq. (3.7)] we find that, in the high noise limit, the $T=0$ dynamic freezing transition takes place at the critical coupling

$$\tilde{J}_d\sim\frac{\hbar\alpha^{5/2}}{M}\exp(-\pi\alpha). \tag{3.38}$$

Thus, for $\alpha\gg 1$, $\tilde{J}_d$ is proportional to the exponentially small energy scale of Eq. (2.21) associated with incoherent tunneling in the isolated TLS's. It must be emphasized that the existence of this scale is a feature of the spherical model used in this paper. Real TLS's (i.e., described by Ising spins) localize at $\alpha=1$. Therefore, $\tilde{J}_d$ is expected to vanish *precisely* at $\alpha=1$ for discrete spins.

Deep in the ordered phase the system is expected to freeze with $q_{EA}\approx 1$. This regime occurs for sufficiently high values of $\alpha$ or sufficiently low values of $\Gamma$. Consider first the former case with $\Gamma\alpha^2\gg 1$. Then, $\epsilon\ll 1$ and we can still use Eq. (3.34) which, for $q_{EA}\approx 1$, reduces to

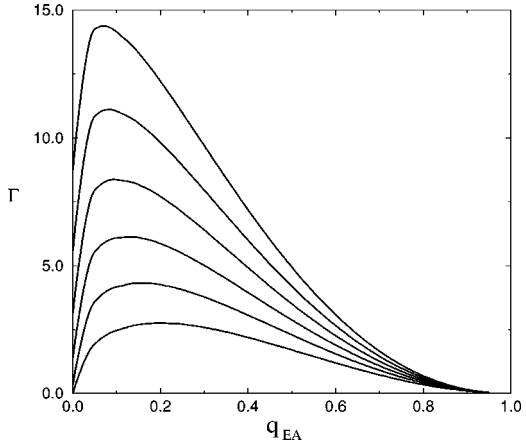


FIG. 7. $\Gamma$ as a function of $q_{EA}$ at $T=0$ for $p=3$ and a sub-Ohmic bath, $s=1/2$ from Eq. (3.29). The coupling $\alpha_{1/2}$ runs from 0 to 2 in intervals of 0.4 from bottom to top.

$$q_{EA} \approx 1 - \frac{1}{\pi\alpha} \ln\left(\frac{\Gamma\alpha^2}{\kappa_p(1)}\right), \quad \Gamma\alpha^2 \gg 1, \tag{3.39}$$

where $\kappa_p(1)=\sqrt{p(p-1)/2}$.

In the opposite case, $\Gamma\alpha^2 \ll 1$, $\epsilon$ is large. In this case

$$g_1(\epsilon) = \frac{2}{3\sqrt{\epsilon}}\left(1 - \frac{3}{8\sqrt{\epsilon}} + \cdots\right), \tag{3.40}$$

leading to

$$q_{EA} \approx 1 - \frac{4}{3\pi}\left(\frac{\Gamma}{\kappa_p(1)}\right)^{1/2}\left[1 - \frac{3}{8}\left(\frac{\Gamma}{\kappa_p(1)}\right)^{1/2}\alpha + \cdots\right], \quad \Gamma\alpha^2 \ll 1. \tag{3.41}$$

In both regimes the effect of the noise leads to an increase in $q_{EA}$, thus stabilizing the ordered phase.

*b. Sub-Ohmic case*. Figure 7 shows $\Gamma$ as a function of $q_{EA}$ for $p=3$ and several values of the coupling to a sub-Ohmic bath with $s=1/2$. The results were obtained by numerically solving Eq. (3.29). The qualitative features of these curves are similar to those found in the Ohmic case.

As discussed in Sec. II, in the sub-Ohmic case the isolated TLS has a localization transition at a critical value $\alpha^{CRIT}$ of the coupling to the bath. We thus expect a transition to the ordered phase at $\tilde{J}=0$ for all $\alpha > \alpha^{CRIT}$ in the interacting system. Near the critical point at $\tilde{J}=0$, $\epsilon$ is small. For $s<1$ the integral on the right-hand side of Eq. (3.30) is finite at $\epsilon=0$ and $g_s(0)=f_s(0)/2$ where $f_s$ is the function defined in Eq. (2.20). Detailed inspection of the behavior of $g_s(\epsilon)$ shows that, as $\epsilon \to 0$,

$$g_s(0) - g_s(\epsilon) \propto \begin{cases} \epsilon & \text{for } 0<s<1/2, \\ \epsilon \ln(1/\epsilon) & \text{for } s=1/2, \\ \epsilon^{\frac{1-s}{s}} & \text{for } 1/2<s<1. \end{cases} \tag{3.42}$$

We consider for simplicity the case $s<1/2$ and take $p=3$ for concreteness. For $\alpha \sim \alpha^{CRIT}$, Eq. (3.30) acquires the form

$$\frac{\tilde{J}M}{\hbar^2}\sqrt{q_{EA}} \propto 1 - \left(\frac{\alpha}{\alpha^{CRIT}}\right)^{1/(2-s)} (1-q_{EA}), \tag{3.43}$$

where $\alpha^{CRIT}$ is given in Eq. (2.22). There is a maximum at $q_{EA} \propto (\tilde{J}M/\hbar^2)^2$. The dynamic transition thus takes place at

$$\tilde{J}_d \propto \frac{\hbar^2}{M}\left(1 - \frac{\alpha}{\alpha^{CRIT}}\right)^{1/2}. \tag{3.44}$$

The jump of the order parameter at the transition is $q^{\star}_{EA} \propto (1-\alpha/\alpha^{CRIT})$. Therefore, for $\alpha=\alpha^{CRIT}$ the dynamic transition is *continuous*. Summarizing, for $\alpha<\alpha^{CRIT}$ the transition between PM phase and SG phase occurs at a finite value of $J_d$ while for $\alpha>\alpha^{CRIT}$ an infinitesimal $\tilde{J}$ is enough to render the system glassy. We expect to obtain this same behavior for an interacting TLS in an Ohmic bath.

At large couplings, $\alpha \gg \alpha^{CRIT}$, $q_{EA} \sim 1$ and we find

$$q_{EA} \approx 1 - \left(\frac{\alpha^{CRIT}}{\alpha}\right)^{1/(2-s)}. \tag{3.45}$$

Notice the absence of $\tilde{J}$-dependent corrections that appear at higher order ($\alpha^{-2}$).

In the opposite limit (large $\tilde{J}$), $\epsilon$ is large. Then,

$$g_s(\epsilon) = \frac{2}{3\sqrt{\epsilon}}(1 - a_s \epsilon^{(s/2-1)} + \cdots), \tag{3.46}$$

with $a_s$ a constant. We find

$$q_{EA} \approx 1 - \frac{4}{3\pi}\left(\frac{\Gamma}{\kappa_p(1)}\right)^{1/2} \times \left[1 - a_s \frac{\Gamma^{s/2}}{\kappa_p^{1-s/2}(1)}\left(\frac{\hbar\omega_{ph}}{\tilde{J}}\right)^{1-s} \frac{\alpha}{\sin\frac{\pi s}{2}} + \cdots\right]. \tag{3.47}$$

As before, the presence of noise favors the ordered phase. The comparison of Eqs. (3.39) and (3.45) shows that, at strong coupling, an Ohmic bath is more effective than a sub-Ohmic bath in freezing the spins. At weak coupling we have a linear dependence on $\alpha$ in both cases. For $\Gamma \ll 1$, however, the slope is higher in the latter case which results now in higher values of $q_{EA}$. Notice the presence of the extra factor $(\hbar\omega_{ph}/\tilde{J})^{1-s}$, which amplifies this effect if the phonon energy is larger than the magnetic energy.

*c. Super-Ohmic case*. In the super-Ohmic case no localization transition exists at $\tilde{J}=0$. For $s>1$, $g_s(\epsilon)$ diverges as $\epsilon^{(1-s)/s}$ in the limit $\epsilon \to 0$. This corresponds to small $\tilde{J}$ or large $\alpha_s$. A calculation similar to those performed above yields the critical coupling

$$\tilde{J}_d \sim \hbar\omega_{ph}\left(\frac{\sin\frac{\pi s}{2}}{\alpha}\right)^{s-1}, \quad \alpha \gg 1. \tag{3.48}$$

As in the Ohmic case, the critical coupling decreases with increasing $\alpha$ but only as a power law. The jump of the order parameter at the transition is however independent of $\alpha$.

Deep in the ordered phase, for small values of $\tilde{J}$, we find

$$q_{EA} \sim 1 - \left(\frac{\tilde{J}_d}{\hbar\omega_{ph}}\right)^{(1-s)/s}\left(\frac{\sin\frac{\pi s}{2}}{\alpha}\right)^{s-1}. \tag{3.49}$$

For small values of $\alpha$ Eq. (3.47) is still valid. Notice that for $s>1$ the enhancement of the order parameter due to the coupling to the bath decreases when $\omega_{ph}/\tilde{J}$ increases.

### E. Real-time correlation function

In thermodynamic equilibrium the correlation function and the imaginary part of the susceptibility are related by

$$C(t) \equiv \frac{1}{N}\sum_i \langle s_i(t)s_i(0)\rangle = q_{EA} + \hbar\int_0^\infty \frac{d\omega}{\pi}\chi''_{REG}(\omega) \times \coth(\beta\hbar\omega/2)\cos(\omega t). \tag{3.50}$$

If instead of the equilibrium response function we use in Eq. (3.50) the expression for $\chi''(\omega)$ obtained through the AMS, we obtain a correlation function that is closely related to the *stationary* part of that obtained through real-time dynamical calculations. This relationship was discussed extensively in CGS in the case of the isolated system with the following conclusions.

(i) The temperature $T_d$ below which the AMS solution exists coincides precisely with the dynamical critical temperature obtained from the dynamical calculations. This is the temperature below which the real-time dynamics of the system becomes nonstationary and violations of the FDT set in.

(ii) The parameter $m$ precisely coincides with $X$, the FDT violation factor. This is related to the *effective* temperature of the system in the aging regime, $T_{\rm eff}=T/X$ (Ref. 37); see Sec. IV.

(iii) The response function derived from the AMS is identical to the out-of-equilibrium response function when the long waiting time is taken first and the weak-coupling limit in taken later on. More precisely,

$$C_{\rm AMS}(t) \equiv \frac{1}{N}\sum_i \langle s_i(t)s_i(0)\rangle_{\rm AMS} = \lim_{\alpha\to 0}\lim_{t_w\to\infty} C_{DYN}(t+t_w,t_w). \tag{3.51}$$

A proof of the analogous properties for the system coupled to the bath can be given following the same lines. The first two conclusions remain unchanged. The third one generalizes to

$$C_{\rm AMS}(t) = \lim_{t_w\to\infty} C_{DYN}(t+t_w,t_w), \tag{3.52}$$

valid for all values of $\alpha$. The aging regime $t \gg t_w$ in which $C_{DYN}(t+t_w,t_w)$ decreases below $q_{EA}$ is not accessible in this approach.

In this section we shall analyze in detail several time regimes in $C(t)$. We use throughout this section the original variables of the problem.

#### 1. No coupling to the bath

We consider first the case in which there is no coupling to a bath. Then, the analytic continuation of Eq. (3.22) is

$$\chi''_{REG}(\omega) = \frac{\omega}{2\kappa_p^2}\left(\frac{M}{\tilde{J}^3}\right)^{1/2}\sqrt{4\kappa_p - \frac{\omega^2 M}{\tilde{J}}}. \tag{3.53}$$

Substituting this expression in Eq. (3.50) and making the change of variables $\omega = \sqrt{4\kappa_p\tilde{J}/M}\ x$ in the integrals we obtain the correlation function

$$C(t) = q_{EA} + \frac{2\hbar}{\pi\kappa_p}\left(\frac{4\kappa_p}{M\tilde{J}}\right)^{1/2}\int_0^1 dx\, x\sqrt{1-x^2} \times \cos(xt/t_0)\coth\left(\frac{\hbar}{2Tt_0}x\right), \tag{3.54}$$

where $t_0$ is a characteristic time given by

$$t_0 = \left(\frac{M}{4\kappa_p\tilde{J}}\right)^{1/2}. \tag{3.55}$$

At $T=0$ Eq. (3.54) reduces to

$$C(t) = q_{EA} + \frac{2\hbar}{\pi\kappa_p}\left(\frac{4\kappa_p}{M\tilde{J}}\right)^{1/2} \times \int_0^1 dx\, x\sqrt{1-x^2}\cos(xt/t_0) = q_{EA} + \frac{2\hbar}{3\pi\kappa_p}\left(\frac{4\kappa_p}{M\tilde{J}}\right)^{1/2} \times {}_1F_2(1;1/2,5/2;-(t/t_0)^2/4), \tag{3.56}$$

where ${}_1F_2$ is a generalized hypergeometric function. From the normalization condition $C(t)=1$ we find the quantum equation of state

$$\kappa_p(1-q_{\rm EA}) = \frac{2\hbar}{3\pi}\left(\frac{4\kappa_p}{M\tilde{J}}\right)^{1/2}, \tag{3.57}$$

found previously in CGS. The asymptotic behavior of the correlation function in the long-time limit is

$$C(t) \overrightarrow{t\gg t_0}\, q_{EA} + \frac{2\hbar}{3\pi\kappa_p}\left(\frac{4\kappa_p}{M\tilde{J}}\right)^{1/2}\left(\frac{t_0}{t}\right)^{3/2} f(t/t_0), \tag{3.58}$$

where $f$ is an oscillatory function that can be expressed in terms of Fresnel integrals. From Eqs. (3.57) and (3.55) the frequency of the oscillations is

$$\omega_0 \sim \frac{\hbar}{M(1-q_{EA})}. \tag{3.59}$$

At the dynamic transition point $q_{EA}$ depends only on $p$. Then, $\omega_0 \propto \hbar/M$, the characteristic frequency of the noninteracting TLS's. Deep in the ordered phase $q_{EA} \approx 1$ and Eq. (3.57) yields $1-q_{EA} \sim \hbar/\sqrt{M\tilde{J}}$. Then, in this limit $\omega_0 \sim \sqrt{\tilde{J}/M}$ .

At temperatures higher than $T_{cr} = \hbar/t_0 \sim \hbar\sqrt{\tilde{J}/M}$ , but low so that the results from the approximation can still be used, we can approximate $\coth z \sim z^{-1}$ in the integral on the right-hand side of Eq. (3.54) and write

$$C(t) \sim q_{EA} + \frac{4T}{\pi\tilde{J}\kappa_p}\int_0^1 dx\sqrt{1-x^2}\cos\left(\frac{xt}{t_0}\right)$$

$$= q_{EA} + \frac{2T}{\tilde{J}\kappa_p} J_1\left(\frac{t}{t_0}\right)\frac{t_0}{t}, \tag{3.60}$$

where $J_1(x)$ is the Bessel function. Notice that Eq. (3.60) also holds for *all* temperatures for times $t \gg \hbar/T$. The normalization condition now yields

$$\kappa_p(1-q_{\mathrm{EA}}) = \frac{4T}{\pi\tilde{J}}\int_0^1 dx\sqrt{1-x^2} = \frac{T}{\tilde{J}}, \tag{3.61}$$

which is the *classical* equation for $q_{\mathrm{EA}}$.[38] In this classical regime the long-time asymptotic behavior of the correlation function is

$$C(t) \overrightarrow{_{t\gg t_0}} q_{EA} + \frac{2T}{\tilde{J}\kappa_p}\sqrt{\frac{2}{\pi}}\left(\frac{t_0}{t}\right)^{3/2}\cos\left(\frac{3\pi}{4} - \frac{t}{t_0}\right). \tag{3.62}$$

Notice that the power-law decay of the amplitude of the oscillations $\propto t^{-3/2}$ at high and low temperatures is the same.

#### *2. Finite coupling to a bath*

In the presence of a coupling to an Ohmic bath there are two different regimes. At frequencies higher than $\omega^\star = \hbar\alpha/M$ the inertial term in Eq. (3.22) dominates over the term proportional to $\alpha$. For times shorter than $t^\star = 1/\omega^\star$ the system thus behaves as if it were isolated. At longer times, when inertia may be ignored, we have

$$\chi''(\omega) \sim \frac{1}{\hbar}\frac{\sqrt{\alpha\omega}}{\alpha\omega + 2\kappa_p\tilde{J}/\hbar}\left(\frac{\hbar}{2\kappa_p\tilde{J}}\right)^{1/2} \tag{3.63}$$

and the motion is overdamped. The correlation function then reads

$$C(t) \overrightarrow{_{t\gg t^\star}} q_{EA} + \frac{2\hbar\sqrt{\gamma_0}}{\pi(2\kappa_p\tilde{J})^{3/2}}\int_0^\infty d\omega\sqrt{\omega}\cos\omega t\coth(\beta\hbar\omega/2), \tag{3.64}$$

where $\gamma_0 = \alpha\hbar$ is the classical friction coefficient. Performing the integral we find

$$C(t) - q_{EA} \overrightarrow{_{t\gg t^\star}} \frac{2\hbar\sqrt{\gamma_0/\pi}}{(4\kappa_p\tilde{J})^{3/2}} \times \begin{cases} -t^{-3/2}, & T=0, \\ 4T/\hbar t^{-1/2}, & T \gg \hbar/t. \end{cases} \tag{3.65}$$

Notice the difference in sign between the results at zero and finite temperature. At zero temperature $C(T)$ approaches $q_{EA}$ from below, whereas at $T \neq 0$ it does so from above. In the Ohmic case the exponent controlling the decay of the $T=0$ correlation function is the same that controls the amplitude of the coherent oscillations found in the absence of noise.

At finite temperature the decay is slower, $C(t) - q_{EA} \propto t^{-1/2}$ . In the classical model, the nonequilibrium symmetrized correlation function $C(t+t_w, t_w)$ approaches the plateau $q_{EA}$ as $C(t+t_w,t_w) - q_{EA} \propto t^{-\nu(T)}$ for $t \ll t_w$. It was found[39] that the temperature-dependent exponent $\nu(T)$ approaches 1/2 in the zero temperature limit in agreement with our result. The calculation of the temperature corrections to the exponent lies beyond the power of our low-temperature approximation.

At finite temperature, in the long-time limit, our results coincide with those obtained from the solution of the classical Langevin equation without inertia. Although the asymptotic form of the correlation function is independent of $M$ (i.e., of the tunneling frequency $\Delta$), it must be remembered that Eq. (3.65) only holds for times longer than $t^\star$ which does depend on $\Delta$. A consequence of this fact is that the dynamics of the model in the limit $\Delta \to 0$ is trivial. Indeed, it can be shown from Eq. (3.22) that

$$\chi''_{REG}(\omega) \overrightarrow{_{M\omega/\gamma_0 \gg 1}} \frac{\gamma_0}{M^2\omega^3}. \tag{3.66}$$

Then, for any finite $\omega$,

$$\lim_{M/\gamma_0 \to \infty} \chi''_{REG}(\omega) \equiv 0. \tag{3.67}$$

However $\chi''_{REG}(\omega)$ cannot be identically zero since the static susceptibility $\chi_{REG}(0)$ is finite and it is given by $\chi_{REG}(0) = \kappa_p^{-1}$ according to Eq. (3.22). Here $\chi_{REG}(0)$ can also be expressed as

$$\chi_{REG}(0) = \int_{-\infty}^{\infty}\frac{d\omega}{\pi}\frac{\chi''_{REG}(\omega)}{\omega}. \tag{3.68}$$

Equations (3.67) and (3.68) are compatible only if

$$\lim_{M/\gamma_0 \to \infty} \frac{\chi''_{REG}(\omega)}{\omega} = \frac{\pi}{\kappa_p}\delta(\omega). \tag{3.69}$$

Therefore, the system has no intrinsic dynamics in this limit. In terms of the original spin model this is a simple consequence of the form of our starting Hamiltonian, Eq. (2.4): if $\Delta = 0$, the spin variables commute with the Hamiltonian and are thus constants of the motion. In terms of the particle

interpretation the limit $M/\gamma_0 \to \infty$ corresponds to an infinitely massive particle that is not able to move or to the limit of zero friction where there is no dissipation.

The expressions in Eq. (3.65) can be readily generalized to non-Ohmic baths. We find that in the long-time limit

$$C(t)-q_{EA} \propto \begin{cases} \cos\left(\frac{s+2}{4}\pi\right) t^{-(1+s/2)}, & T=0, \\ \cos\left(\frac{s}{4}\pi\right) t^{-s/2}, & T \gg \hbar/t. \end{cases} \tag{3.70}$$

## IV. REAL-TIME DYNAMICS

In this section we study the real-time dynamics of the system coupled to the environment. We use the dynamic equations for the symmetrized correlation and linear response functions derived in Ref. 23 with the Schwinger-Keldysh formalism and we solve them numerically, as a function of time, for different couplings to the bath and different environments. We compare the results to the ones obtained in the previous section with the imaginary time formalism.

### A. Dynamic equations

The dynamic equations for the model defined in Sec. II were derived in Ref. 23. They are of the Schwinger-Dyson form and read

$$[M\partial_t^2 + z(t)]R(t,t') = \delta(t-t') + \int_0^\infty dt''\, \Sigma(t,t'')R(t'',t'), \tag{4.1}$$

$$[M\partial_t^2 + z(t)]C(t,t') = \int_0^\infty dt''\, \Sigma(t,t'')C(t'',t') + \int_0^{t'} dt''\, D(t,t'')R(t',t''), \tag{4.2}$$

with the equal-time conditions $C(t,t)=1$ and $R(t,t)=0$ and

$$\lim_{t' \to t^-} \partial_t R(t,t') = \frac{1}{M},$$

$$\lim_{t' \to t^+} \partial_t R(t,t') = 0, \tag{4.3}$$

$$\lim_{t' \to t^-} \partial_t C(t,t') = \lim_{t' \to t^+} \partial_t C(t,t') = 0. \tag{4.4}$$

The symmetrized correlation function is defined as $C(t,t') \equiv 1/(2N)\Sigma_i \langle \hat{s}_i(t)\hat{s}_i(t') + \hat{s}_i(t')\hat{s}_i(t)\rangle$. The equation for the Lagrange multiplier $z(t)$ reads

$$z(t) = \int_0^t dt''[\Sigma(t,t'')C(t,t'') + D(t,t'')R(t,t'')] + M\int_0^t dt'' \int_0^t dt'''[\partial_t R(t,t'')]D(t'',t''')[\partial_t R(t,t''')] + M^2[\partial_t R(t,s)\partial_{st}^2 C(s,t) - \partial_{st}^2 R(t,s)\partial_{t'} C(s,t')]\big|_{\substack{s\to 0 \\ t\to t'}}. \tag{4.5}$$

The total self-energy and vertex include the interaction with the bath and are given by

$$\Sigma(t,t') \equiv -4\eta(t-t') - \frac{p\tilde{J}^2}{\hbar}\mathrm{Im}\left[C(t,t') - \frac{i\hbar}{2}R(t,t')\right]^{p-1}, \tag{4.6}$$

$$D(t,t') \equiv 2\hbar\nu(t-t') + \frac{p\tilde{J}^2}{2}\mathrm{Re}\left[C(t,t') - \frac{i\hbar}{2}[R(t,t') + R(t',t)]\right]^{p-1}, \tag{4.7}$$

with

$$\nu(t-t') = \int_0^\infty d\omega I(\omega)\coth\left(\frac{1}{2}\beta\hbar\omega\right)\cos[\omega(t-t')], \tag{4.8}$$

$$\eta(t-t') = -\theta(t-t')\int_0^\infty d\omega\, I(\omega)\sin[\omega(t-t')]. \tag{4.9}$$

The spectral density of the bath, $I(\omega)$, has been defined in Eq. (2.11).[40]

In the following we shall compare the effect of environments with different values of $s$ and using different coupling strengths. The high-frequency cutoff $\omega_c$ is introduced to avoid the divergence of $\nu(\tau)$. In the sub-Ohmic case, when we solve the equations numerically, we also need a low-frequency cutoff, which we impose in a hard manner by including a factor $\theta(\omega-b)$ in the definition of $I(\omega)$.

The kernels $\nu$ and $\eta$ can be computed for all values of $s$. In the numerical solution to the set of coupled integro-differential equations (4.1) and (4.2) it is more useful to use the integral of the kernel $\eta$, $\hat{\eta}(\tau) \equiv \int_\tau d\tau'\, \eta(\tau')$, which reads

$$\hat{\eta}(\tau) = \frac{\alpha\hbar}{2\pi}\frac{\omega_c}{(1+\omega_c^2\tau^2)^{s/2}}\cos[s\arctan(\omega_c\tau)]\Gamma(s) \tag{4.10}$$

and, when $s$ takes the values 1/2,1,3/2, it becomes

$$\hat{\eta}(\tau) \sim \begin{cases} \sqrt{\frac{\omega_c}{\tau}} & s=1/2 \quad \text{sub-Ohmic}, \\ \frac{1}{\tau} & s=1 \quad \text{Ohmic}, \\ \frac{1}{\sqrt{\omega_c\tau^3}} & s=3/2 \quad \text{super-Ohmic}. \end{cases}$$

On the right-hand side we have written the limiting form for $\omega_c \tau \gg 1$. It is clear that, as for the imaginary-time kernels, the dependence on $\omega_c$ is very different in each of these cases.

We shall rescale the real time and the other parameters and functions in the dynamic equations to match the definitions that we used in the Matsubara calculation. Under the rescaling of time, $t \to \tilde{J}/\hbar t$, the symmetrized correlation function remains unchanged and the response transforms as $R \to \hbar R$. The rescaled dynamic equations are identical to Eqs. (4.1) and (4.2) with $M$ replaced by $\Gamma^{-1}$.

### B. Numerical study of the real-time dynamics

As shown in Sec. III B, both static and dynamic transition lines depend strongly on the strength of the coupling between system and bath. We can also see this effect by following the real-time dynamics of the system coupled to the environment. We have solved Eqs. (4.1) and (4.2) numerically with a predictor-corrector algorithm that allows us to reach long times with a high accuracy. For each set of parameters we have checked the data collapse for different values of the iteration step $h$ in the discretized equations. In general, there is a good collapse for $h \leqslant 0.02$ and, typically, we have used $h=0.01$ and $h=0.02$.

#### *1. Effect of the interactions: Localization against glassy behavior*

In the Introduction and Sec. I we recalled several results for localization in dilute two-level systems coupled to a bath. In this paper we focus on a soft spin version of the interacting problem. Our first aim is to determine the effect of the coupling $\tilde{J}$ on the localization properties of this system from a real-time dynamic point of view. In Fig. 8 we show the decay of the symmetrized correlation $C(t+t_w, t_w)$ using a sub-Ohmic bath with $s=0.5$, $\omega_c=10$, and $\omega_{ph}=5$. The three upper curves were obtained for $\alpha=4$ and changing the value of the SG coupling strength $\tilde{J}$. When $\tilde{J}=0$ the system localizes for $\alpha > \alpha^{CRIT}$: for any $t_w$ and long enough $t$ the symmetrized correlation reaches a plateau and it does not decay below this value. When a small coupling is switched on the decay changes. The symmetrized correlation approaches a plateau for small values of $t-t_w$ but it subsequently leaves the plateau and decays towards zero. The system has glassy nonequilibrium dynamics that we shall quantify below. Finally, when the coupling to the bath is very small and $\tilde{J}=0$ the system does not localize and the symmetrized correlation decays to zero with broad oscillations.

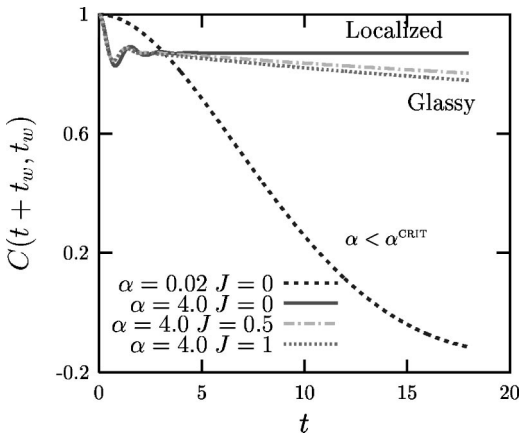


FIG. 8. The decay of the symmetrized correlation at $T=0$ in three cases: localization for $\alpha=4$ and $\tilde{J}=0$, glassy decay for two nonvanishing values of $\tilde{J}$, $\tilde{J}=0.5$, and $\tilde{J}=1$, and a simple decay towards zero for the case of a small coupling to the bath, $\alpha=0.2$ and $\tilde{J}=0$. We have chosen a sub-Ohmic bath with $s=0.5$, $\omega_{ph}=5$ and $\omega_c=10$. The quantum parameter $\Gamma$ equals 1.

#### *2. Dynamics in the paramagnetic phase*

For a chosen coupling to a bath, at sufficiently high values of $\Gamma$ and/or $T$ the system equilibrates with the environment and it quickly reaches a stationary regime where the quantum FDT is satisfied. This property has been proved for the $p$-spin model in Ref. 23, for the large-$N$ fully connected Heisenberg SU($N$) model in Ref. 29, and for a soft version of the quantum model in Ref. 30. In all cases the systems were coupled to an Ohmic environment and the limit of weak coupling, $\lim_{\alpha \to 0} \lim_{t_w \to \infty}$, was considered. The symmetrized correlation and response have a rapid decay towards zero with oscillations that depend on the value of the quantum parameter $\Gamma$ and, as we show here, on the coupling to and the type of environment used.

We first consider a fixed Ohmic environment; i.e., we take $s=1$ and we fix $\omega_c=10$. We display in Fig. 9 the decay of the symmetrized correlation and response functions for different values of $\Gamma$ in the PM phase. It is clear from the figure that the period of the oscillations decreases with $\Gamma$. In order to quantify this dependence one can compute $\chi''(\omega)/\omega$ and follow the evolution of the peaks. We show two examples in

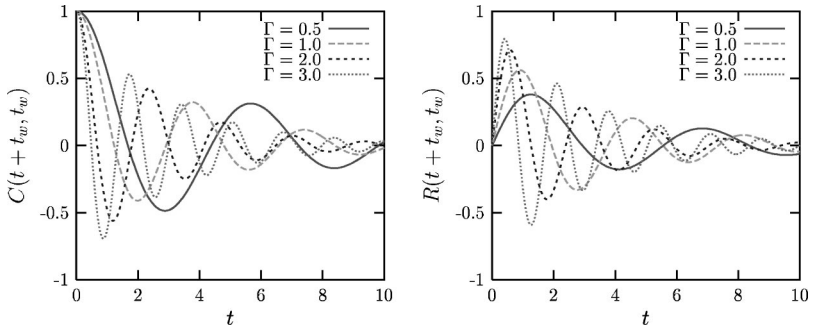


FIG. 9. The stationary symmetrized correlation (left) and response (right) functions at $T=2$ for several values of the quantum parameter $\Gamma$, given in the key. The bath is Ohmic and $\omega_c=5$, $\alpha=0.8$.

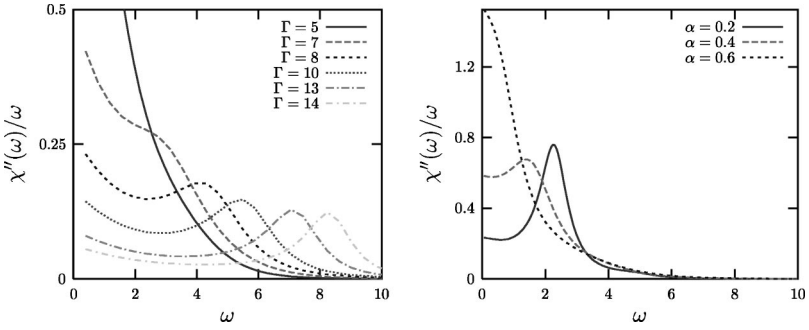


FIG. 10. The frequency dependence of $\chi''(\omega)/\omega$. Left panel: $T=0$, $\alpha=0.6$, $\omega_c=5$, and several values of $\Gamma$. Right panel: $\Gamma=5$, $T=0$, $\omega_c=10$, and several values of $\alpha$. The environment is Ohmic in both cases.

Fig. 10. The data in the left panel correspond to those in Fig. 9. In the right panel we represent $\chi''(\omega)/\omega$ for $T=0$, $\Gamma=5$, and several values of $\alpha$. For small values of $\alpha$ the system is deep in the PM phase and there is a well-defined peak in $\chi''(\omega)/\omega$ at a finite value $\omega_0$ that increases with decreasing $\alpha$. At high enough values of $\alpha$ a tail at low frequencies starts developing, indicating that the dynamics is slower and that the system approaches the transition towards the glassy phase. Eventually, as discussed in Sec. III A, for high enough $\alpha$, the parameters fall below the transition and the system becomes glassy with slow dynamics.

### *3. Dynamics in the glassy phase*

In Fig. 11 we compare the behavior of the symmetrized correlation and response functions in the glassy phase when the system is coupled to an Ohmic environment through different coupling constants. We choose $T=0.1$, $\Gamma=4$, and we compare the effect of $\alpha=0.2$ and $\alpha=1$. The high-frequency cutoff is $\omega_c=5$. From the discussion in Sec. III we expect that the system is in the PM phase in the first case and in the SG phase in the second. This is seen in Fig. 11. For $\alpha=0.2$ the symmetrized correlations rapidly reach a stationary regime and they oscillate around zero. For $\alpha=1$ the behavior is different. There is a first rapid decay towards a plateau that has a low value and, then, a slow and monotonic decay towards zero. Aging effects are apparent from the figure. The response function also shows a qualitatively different behavior according to the value of $\alpha$. In one case it quickly acquires a stationary oscillatory behavior around zero; in the other it has a long tail as expected in a glassy system. We then conclude that the system has undergone a dynamic phase transition between the PM and SG phases at an intermediate value of $\alpha$.

An approximate expression for the dependence of the Edwards-Anderson parameter on $\Gamma$ and $\alpha$, at $T\sim 0$, has been obtained in Sec. III D. We can also check this law by estimating the value of $q_{EA}$ from the numerical solution of the real-time equations. If we plot the symmetrized correlation function for several values of $\alpha$ on a log-log scale the plateau at $q_{EA}$ can be easily identified. It is a slowly growing function of $\alpha$ that is rather well described by Eq. (3.39).

We also investigated the effect of different environments (different $s$) of the same strength (same $\alpha$) using the same value of the high-frequency cutoff that we took equal to $\omega_{ph}$. From the discussion in Sec. III C for some values of $\omega_{ph}$ we expect the relaxation to be slowest for the sub-Ohmic bath, intermediate in the Ohmic case, and faster for a super-Ohmic environment. This is illustrated in Fig. 12. The decay is slower when $s=0.5$ than in the other cases. In the extreme case of $s=4$ the system has gone across the transition towards the PM phase. However, this behavior is not generic.

The relation between the symmetrized correlation and response plays a key role in the description of the dynamic behavior of glassy systems. When the system is in equilibrium, this relation is model independent and it is given by the FDT. When the system is glassy and it evolves out of equilibrium, the conditions to prove the theorem are not satisfied but simple generalizations have been exhibited in a number of models.[38,23]

The quantum FDT for a system in equilibrium, in the rescaled variables, reads

$$R(t)=\theta(t)i\int_{-\infty}^{\infty}d\omega e^{-i\omega t}\tanh\left(\frac{\beta\tilde{J}\omega}{2}\right)\tilde{C}(\omega), \quad (4.11)$$

where

$$\tilde{C}(\tilde{\omega})=2\,\mathrm{Re}\int_{0}^{\infty}d\tau e^{i\omega t}C(\tau). \quad (4.12)$$

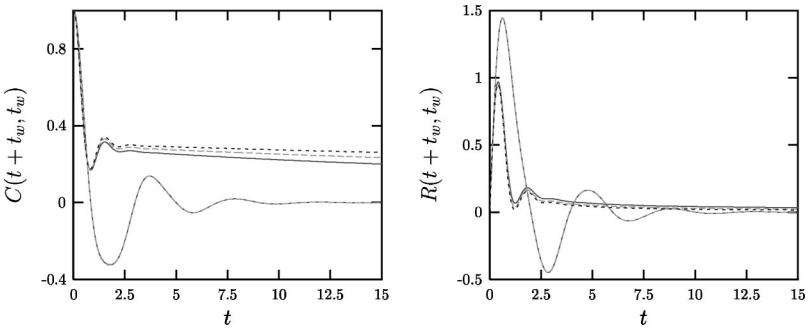


FIG. 11. Left: the symmetrized correlation $C(t+t_w,t_w)$ as a function of $t$ for $\alpha=0.2$ (PM phase) and $\alpha=1$ (SG phase). The temperature is $T=0.1$ in both cases. The different curves correspond to different waiting times $t_w=5,10,20$. For $\alpha=0.2$ the curves collapse on an asymptotic one, while for $\alpha=1$ they show aging effects. Right: the response $R(t+t_w,t_w)$ as a function of $t$ for the same parameters. The effect is similar.

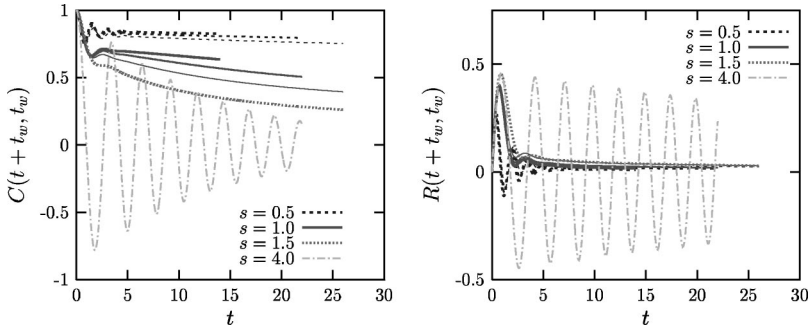


FIG. 12. The symmetrized correlation and the linear response at $T=0.1$, for $\Gamma=1$. We compare the effect of a sub-Ohmic ($s=0.5$), an Ohmic ($s=1$), and a two super-Ohmic ($s=1.5$, $s=4$) baths. See the key for the details. The coupling to the bath is kept fixed to $\alpha=3$ and the high-frequency cutoff equals the phonon frequency, $\omega_c=\omega_{ph}=5$.

The quantum FDT is an integral relation between the stationary linear response and the symmetrized correlation function.

The asymptotic dynamics in the glassy phase take place in two time scales that are separated by the plateau in the symmetrized correlation function. As shown in Ref. 23 for the weak-coupling limit, the stationary part of the decay, when the symmetrized correlation decays from 1 to $q_{EA}$, is such that the quantum FDT holds. We have checked that this result also holds when the system is strongly coupled to a non-Ohmic bath. In the weak-coupling limit, when the symmetrized correlation decays beyond $q_{EA}$, the relation between linear response and symmetrized correlations takes the form of the classical FDT and it reads

$$R(t)=\theta(t)\beta_{EFF}\tilde{J}\frac{\partial}{\partial t}C(t), \tag{4.13}$$

where $\beta_{EFF}$ is the inverse of an effective temperature[37] $T_{EFF}$ and $\tilde{J}$ appears since we have rescaled time. A concrete way of testing the validity of this equation is to plot the integrated response function

$$\chi(t+t_w,t_w)\equiv\int_{t_w}^{t+t_w}dt'R(t+t_w,t') \tag{4.14}$$

against the symmetrized correlation $C(t+t_w,t_w)$ for a long enough $t_w$ and using $t$ as a parameter. For short time differences, when $t-t_w\ll t_w$ and $C(t+t_w,t_w)>q_{EA}$, this construction does not have any particular meaning and the curve is nonmonotonic with strong oscillations. Instead, when $t-t_w\approx t_w$ or longer and $C(t+t_w,t_w)<q_{EA}$, the curve becomes a straight line of slope $-1/T_{EFF}$.

In Fig. 13 we display the $\chi$ against $C$ plots for different values of the parameters, explained in the caption and keys. The panel on the left shows the $\chi$ vs $C$ curve for different values of the coupling $\alpha$. The slopes of the curves, and hence $T_{EFF}$, change smoothly and there is a clear nontrivial dependence on this parameter. The panel on the right displays the $\chi(C)$ plot for a fixed value of the coupling $\alpha$ and several values of $s$, $s=1,1.5,4$. The first two cases are in the glassy phase while the latter falls in the PM phase and the parametric plot does not show a straight line piece. It is difficult to decide from these figures if the slopes depend on $s$ or not.

In order to sharpen our conclusions about the dependence of $T_{EFF}$ on the characteristics of the environment we take profit of the empirical relation between $T_{EFF}$ and the breaking point parameter $m$ in the replica analysis of the same model, $T_{EFF}=T/m$. In Sec. III we developed a low-temperature, low-frequency approximation to solve the saddle point equations stemming from the replicated Matsubara analysis of this problem. In these limits we derived a set of equations that link $T/m$ to $\alpha$ and $s$ that can be solved numerically. We found that for fixed $s$ the effective temperature $T_{EFF}$ is a growing function of $\alpha$. This result is reminiscent to the dependence of $T_{EFF}$ on the external temperature $T$ in a classical problem: the lower $T$, the higher $T_{EFF}$, meaning that higher values of the effective temperature are reached when the system is deeper in the glassy phase. Each curve approaches one when $\alpha\to\infty$ and the corrections can be read from the asymptotic analysis presented in Sec. III. The dependence of $T_{EFF}$ on $s$ is weak but nonmonotonic. (We have already encountered a nonmonotonicity related to the fact that the factor $\omega_{ph}^{1-s}$ changes the coupling between system and bath differently for different values of $s$.)

## V. CONCLUSIONS

In this article we discussed the effect of a quantum environment on the nonequilibrium dynamic properties of an interacting quantum glassy system. We have shown that, as in

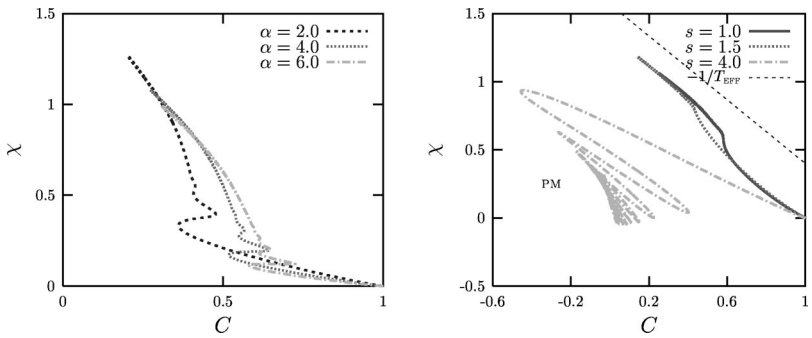


FIG. 13. Left: the parametric $\chi$ against $C$ curves for different values of the coupling to the environment, at fixed $T=0.1$, $\omega_c=5$, and using an Ohmic bath. Right: the dependence of the $\chi$ against $C$ plot on the kind of bath used. We include a straight line as a guide to the eye. In all curves $T=0.1$, $\alpha=2$, and $\omega_c=5$.

the case of a simple TLS, the influence of the quantum bath is very important.

Two limits of the quantum model are easy to derive or were already known. On the one hand, in the absence of interactions, the calculations shown in Sec. II and the numerical results of Sec. IV B 1 prove that when the model is coupled to a sub-Ohmic bath, it undergoes a localization transition at a critical value of the coupling $\alpha$. The localized phase is characterized by a symmetrized two-time correlation function that, as a function of time difference, approaches a nonvanishing asymptotic value and *never* decays to zero. On the other hand, it was known that when interactions are switched on and the limit of weak coupling, $\alpha \to 0$, is taken, the model has glassy dynamics with a symmetrized correlation function that depends on the waiting time and decays in two steps with a first approach to a plateau and a second decay towards zero.[23]

The aim of this article was to analyze the combined effects of the interaction ($\tilde{J} \neq 0$) and a strong coupling ($\alpha \neq 0$) to quantum environments of different types (different $s$). We summarize our findings as follows:

First, we determined if the model has a localized phase in the presence of interactions. How to define such a phase for an interacting system is a difficult question (see, e.g., Ref. 41). Here, we adopted as evidence for a localized phase the fact that for a long enough waiting time $t_w$ the symmetrized correlation function does not decay to zero at any time difference $t - t_w$. With this criterion we saw that, as expected, there is no localized phase when interactions are switched on.

This result can be interpreted *a posteriori* by resorting to the concept of effective temperatures generated by the nonequilibrum dynamics of glassy systems. Indeed, it has been shown for classical systems that the modification of the fluctuation-dissipation theorem observed in systems evolving slowly out of equilibrium is related to the self-generation of effective temperatures (typically higher than the one of the environment).[37] The proof presented in Ref. 37 has not been extended to quantum systems yet. However, as argued in Ref. 23 for the quantum model studied in this paper when weakly coupled to an environment, the slow part of the relaxation looks *classical*, with a quantum fluctuation-dissipation relation that becomes classical with an effective temperature that is higher than the temperature of the environment. In particular, when the model is coupled a quantum bath at zero temperature it acquires a nonvanishing effective temperature. This effect has been observed in other quantum glassy systems too.[29,30] When the system is strongly coupled to the environment the relaxation slows down with respect to the weakly coupled case. However, the two-step relaxation remains with a slow regime controlled by a nonvanishing effective temperature. Thus, we conclude that generation of an effective temperature by the interactions is consistent with the fact that the system does not localize. It is well known that even in simple TLS's the localization effects disappear at finite temperature.

Next, we analyzed the effect of a strong coupling to an environment on the glassy properties of the model. We showed that stronger couplings to the bath favor the glassy phase for any type of bath. By this we mean that for larger value of $\alpha$ the area of the spin-glass phase on the $(T,\Gamma)$ plane increases. We also characterized the dependence on $\alpha$ of several properties of the system as the Edwards-Anderson parameter, the effective temperature, etc. The large-$\alpha$ limit of our model is experimentally realized in Kondo alloys[19,20] where the spins are coupled to conduction electrons through a Kondo interaction $J_K$. The spin-boson model is known to be equivalent to the Kondo model[13] with the identifications $\Delta \propto J_K$ and, in the weak-Kondo-coupling limit, $\alpha \approx 1 - J_K \rho_0$ where $\rho_0$ is the conduction electron density of states at the Fermi level. Therefore, a *decrease* in the Kondo coupling $J_K$ corresponds to an *increase* in the coupling to the bath $\alpha$. Our finding that the extent of the spin glass phase increases with increasing $\alpha$ is then consistent with the Doniach scenario[42] according to which, at $T=0$, the ordered phase (a spin-glass in this case) exists for $\tilde{J} > T_K \propto \exp[-1/(J_K \rho_0)]$. Biroli and Parcollet[29] discussed the $\mathcal{N} \to \infty$ limit of the SU($\mathcal{N}$) Heisenberg disordered model with a Kondo coupling and they also found that the transition temperature decreases with increasing $J_K$.

We also studied the effect of different types of baths. Concerning this issue the conclusions are cumbersome given the fact that a new parameter, the phonon frequency $\omega_{ph}$, appears in the spectral density when $s \neq 1$. If $\omega_{ph}$ is not equal to 1, the effect of different baths is complicated. For instance, the dependence of $q_{EA}$ on $s$ can be nonmonotonic as well as the location of the critical line on the $(T,\Gamma)$ plane. We exhibited some examples but we cannot draw general conclusions concerning this issue.

Finally, an important issue that deserves discussion is the dependence of the order of the transition upon the coupling to the bath, $\alpha$. In the Ohmic case, the jump of the order parameter $q_{EA}$ at $T=0$ decreases with increasing $\alpha$ and vanishes only when $\alpha \to \infty$. Therefore, the tricritical temperature is finite for all $\alpha < +\infty$ and it goes smoothly to zero when $\alpha \to \infty$. Instead, in the sub-Ohmic case, at $T=0$, $q_{EA}$ vanishes at $\alpha = \alpha^{CRIT} < +\infty$ and the transition becomes continuous. As emphasized in Sec. III D 2 we expect $\alpha^{CRIT}$ to be finite for discrete spins when coupled to an Ohmic bath, leading to a suppression of the first-order transition for sufficiently large coupling also in this case.

The motivation for this study were manifold. The effect of quantum environments on interacting macroscopic quantum systems is a problem that is now being revisited in the context of quantum computing.[43] Decoherence, or how quantum interference effects are lost due to the interaction with the environment, has to be as much reduced as possible to make a quantum computer performing. Again in the context of quantum computing, an isolated Edwards-Anderson quantum model in a random transverse field has been proposed to mimic an isolated quantum computer with (short-range) interactions between the spins (that represent qubits) and with static ''imperfections'' in the individual two-level system energies.[44] In this work we analyzed a soft limit of a disordered quantum model with long-range $p > 2$ interactions in a transverse field. It would be very interesting to see which, if any, of our conclusions are modified if the soft spin limit is

lifted and, even more importantly, if a finite-dimensional model is considered. This project, however, is a very difficult one.

On a more physical side, glassy phases at very low temperatures where quantum fluctuations are important have been identified in a number of physical systems. In the proper analysis of these systems the role played by the quantum environment has to be taken into account. Our results are a first step towards the characterization of the effects of the environment. Again, it would be interesting to go beyond the mean-field limit and derive similar results for a finite-dimensional model.

**ACKNOWLEDGMENTS**

We especially thank L. Ioffe for suggesting this problem to us and for discussions at the initial stages of this work. We thank the international collaboration ECOS-Sud for a travel grant and the research program ''Problèmes d'optimization et systèmes désordonnés quantiques'' (ACI Jeunes Chercheurs) for financial support. G.L. is associated with CONICET Argentina and acknowledges Fundación Antorchas for financial support. L.F.C. is supported by ICTP, Trieste, Italy. C.d.S.S. acknowledges financial support from the Portuguese Research Council under Grant Nos. PRAXIS XXI/BPD/16303/98 and SFRH/BPD/5557/2001.

[1] A. J. Leggett *et al.*, Rev. Mod. Phys. **59**, 1 (1987); **67**, 725 (1995).
[2] U. Weiss, in *Series Modern Condensed Matter Physics* (World Scientific, Singapore, 1993), Vol. 2.
[3] A. O. Caldeira and A. J. Leggett, Phys. Rev. Lett. **46**, 211 (1981); Ann. Phys. (N.Y.) **149**, 374 (1983).
[4] A. J. Bray and M. A. Moore, Phys. Rev. Lett. **49**, 1545 (1982).
[5] S. Chakravarty, Phys. Rev. Lett. **49**, 681 (1982); S. Chakravarty and A. J. Leggett, *ibid.* **52**, 5 (1984).
[6] R. P. Feynman and F. L. Vernon, Jr., Ann. Phys. (N.Y.) **24**, 118 (1963).
[7] N. V. Prokof'ev and P. C. E. Stamp, Phys. Rev. Lett. **80**, 5794 (1998).
[8] D. Withof and E. Fradkin, Phys. Rev. Lett. **64**, 1835 (1990).
[9] Q. Si, J. L. Smith, and K. Ingersent, Int. J. Mod. Phys. B **13**, 2331 (1999); K. Ingersent and Q. Si, cond-mat/0109417 (unpublished); and cond-mat/9810226 (unpublished).
[10] A. Sengupta, Phys. Rev. B **61**, 4041 (2000).
[11] S. Chakravarty and J. Rudnick, Phys. Rev. Lett. **75**, 501 (1995).
[12] P. W. Anderson and G. Yuval, Phys. Rev. Lett. **32**, 89 (1969); J. Phys. C **4**, 607 (1971); P. W. Anderson, G. Yuval, and D. R. Hammann, Phys. Rev. B **1**, 4464 (1970).
[13] T. A. Costi and C. Kieffer, Phys. Rev. Lett. **76**, 1683 (1996); T. A. Costi, *ibid.* **80**, 1038 (1998).
[14] F. Guinea, V. Hakim, and A. Muramatsu, Phys. Rev. B **32**, 4410 (1985).
[15] H. Grabert, P. Schramm, and G-L. Ingold, Phys. Rep. **168**, 115 (1988).
[16] A. Caldeira and A. Legget, Phys. Rev. A **31**, 1059 (1985).
[17] B. Golding, N. M. Zimmerman, and S. N. Coppersmith, Phys. Rev. Lett. **68**, 998 (1992).
[18] W. Wu, B. Ellmann, T. F. Rosenbaum, G. Aeppli, and D. H. Reich, Phys. Rev. Lett. **67**, 2076 (1991); W. Wu, D. Bitko, T. F. Rosenbaum, and G. Aeppli, *ibid.* **71**, 1919 (1993); J. Brooke, D. Bitko, T. F. Rosenbaum, and G. Aeppli, Science **284**, 779 (1999).
[19] R. Vollmer, T. Pietrus, H. v. Löhneysen, R. Chau, and M. B. Maple, Phys. Rev. B **61**, 1218 (2000).
[20] Y. Tabata, D. R. Grempel, M. Ocio, T. Taniguchi, and Y. Miyako, Phys. Rev. Lett. **86**, 524 (2001).
[21] A qualitative description of the renormalization-group flows in the vicinity of this quantum transition has been given for a different but much related problem by Q. Si and J. Lleweilun Smith, Phys. Rev. Lett. **16**, 3391 (1996).
[22] Y. Y. Goldschmidt, Phys. Rev. B **41**, 4858 (1990); V. Dobrosavljevic and D. Thirumalai, J. Phys. A **22**, L767 (1990); L. De Cesare, K. Lubierska-Walasek, I. Rabuffo, and K. Walasek, *ibid.* **29**, 1605 (1996); T. Kopeć, Phys. Rev. B **52**, 9590 (1995); T. M. Nieuwenhuizen and F. Ritort, Physica A **250**, 89 (1998).
[23] L. F. Cugliandolo and G. Lozano, Phys. Rev. Lett. **80**, 4979 (1998); Phys. Rev. B **59**, 915 (1999).
[24] L. F. Cugliandolo, D. R. Grempel, and C. A. da Silva Santos, Phys. Rev. Lett. **85**, 2589 (2000).
[25] L. F. Cugliandolo, D. R. Grempel, and C. A. da Silva Santos, Phys. Rev. B **64**, 014403 (2001).
[26] G. Biroli and L. F. Cugliandolo, Phys. Rev. B **64**, 014206 (2001).
[27] A. Crisanti and H-J Sommers, Z. Phys. B: Condens. Matter **87**, 341 (1992).
[28] J-P Bouchaud, L. F. Cugliandolo, J. Kurchan, and M. Mézard, in *Sping-Glasses and Random Fields*, edited by A. P. Young (World Scientific, Singapore, 1998).
[29] G. Biroli and O. Parcollet, Phys. Rev. B **65**, 094414 (2002).
[30] M. Kennett and C. Chamon, Phys. Rev. Lett. **86**, 1622 (2001); M. Kennett, C. Chamon, and Y. Ye, Phys. Rev. B **64**, 224408 (2001).
[31] T. R. Kirkpatrick and D. Thirumalai, Phys. Rev. Lett. **58**, 2091 (1987); Phys. Rev. B **36**, 5388 (1987).
[32] T. Giamarchi and P. Le Doussal, Phys. Rev. B **53**, 15 206 (1996).
[33] A. Georges, O. Parcollet, and S. Sachdev, Phys. Rev. Lett. **85**, 840 (2000); Phys. Rev. B **63**, 134406 (2001).
[34] S. Sachdev, N. Read, and R. Oppermann, Phys. Rev. B **52**, 10 286 (1995); A. M. Sengupta and A. Georges, *ibid.* **52**, 10 295 (1995); D. R. Grempel and M. J. Rozenberg, *ibid.* **60**, 4702 (1999).
[35] H. Ishii and T. Yamamoto, J. Phys. C **18**, 6225 (1985); T. Yamamoto and H. Ishii, *ibid.* **20**, 6053 (1987); J. Miller and D. A. Huse, Phys. Rev. Lett. **70**, 3147 (1993); M. Rozenberg and D. R. Grempel, *ibid.* **81**, 2550 (1998).
[36] P. Shukla and S. Singh, Phys. Lett. **81A**, 477 (1981); T. Vojta, Phys. Rev. B **53**, 710 (1996); T. Vojta and M. Schreiber, *ibid.* **53**, 8211 (1996); S. Sachdev and Y. Ye, Phys. Rev. Lett. **70**, 3339 (1993); N. Read, S. Sachdev, and J. Ye, Phys. Rev. B **52**, 384 (1995).
[37] L. F. Cugliandolo, J. Kurchan, and L. Peliti, Phys. Rev. E **55**, 3898 (1997).
[38] L. F. Cugliandolo and J. Kurchan, Phys. Rev. Lett. **71**, 173 (1993).

[39] L. F. Cugliandolo and P. Le Doussal, Phys. Rev. E **53**, 1525 (1996).

[40] In Ref. 23 the spectral density was defined as $4\bar{M}\gamma_0/\pi(\omega/\Lambda)^{s-1}\omega\exp(-\omega/\Lambda)$. The relation between the constants $\bar{M}\gamma_0$ and $\alpha$ is then $2\bar{M}\gamma_0=\alpha\hbar$.

[41] T. Vojta, F. Epperlein, and M. Schreiber, Phys. Status Solidi B **205**, 53 (1998).

[42] S. Doniach, Physica B **91**, 231 (1977).

[43] C. Miquel, J. P. Paz, and R. Perazzo, Phys. Rev. A **54**, 2605 (1996); C. Miquel, J. P. Paz, and W. Zurek, Phys. Rev. Lett. **78**, 3971 (1997).

[44] B. Georgeot and D. L. Shepelyansky, Phys. Rev. E **62**, 3504 (2000); **62**, 6366 (2000).